UNIVERSIDADE DE SÃO PAULO
INSTITUTO DE FÍSICA DE SÃO CARLOS

KAREN JOCHELAVICIUS

Effects caused by water-soluble chitosans with high molecular weight in bacterial and mammal membrane models using Langmuir monolayers

São Carlos
2022

KAREN JOCHELAVICIUS

Effects caused by water-soluble chitosans with high molecular weight in bacterial and mammal membrane models using Langmuir monolayers

Thesis presented to the Graduate Program in Physics at the Instituto de Física de São Carlos, Universidade de São Paulo to obtain the degree of Doctor of Science.

Concentration area: Biomolecular Physics
Advisor: Prof. Dr. Osvaldo Novais de Oliveira Junior

Corrected Version
(Original version available on the Program Unit)

São Carlos
2022

I AUTHORIZE THE REPRODUCTION AND DISSEMINATION OF TOTAL OR PARTIAL COPIES OF THIS DOCUMENT, BY CONVENTIONAL OR ELECTRONIC MEDIA FOR STUDY OR RESEARCH PURPOSE, SINCE IT IS REFERENCED.

Jochelavicius, Karen
Effects caused by water-soluble chitosans with high molecular weight in bacterial and mammal membrane models using Langmuir monolayers / Karen Jochelavicius; advisor Osvaldo Novais de Oliveira Junior - corrected version -- São Carlos 2022.
62 p.

Thesis (Doctorate - Graduate Program in Biomolecular Physics) -- Instituto de Física de São Carlos, Universidade de São Paulo - Brasil , 2022.

1. Langmuir monolayers. 2. Chitosan. 3. Bactericide activity. I. Oliveira Junior, Osvaldo Novais de, advisor. II. Title.

ACKNOWLEDGEMENTS

I would like to thank everyone and everything that directly or indirectly influenced me and helped me to complete my doctorate studies: family, friends, professors, boyfriend, colleagues, collaborators, people that inspires me, the institute, the institute's library and librarians, the university, funding agencies, dance and arts in general… In especial, I would like to thank my advisor, who is of an immense knowledge and very supportive. Plus, revises your work as fast and soon as one can imagine. Thank you! In addition, I would like to thank Thaty, who was the first to advise me and believe in me, and who taught me almost everything, and Andressa, who started the studies with the class of chitosans I used in this work, and helped me a lot! Above all, I would like to thank science and, further, scientists, especially Brazilian. I finished my studies in a scenario of Covid-19 pandemics (thankfully, now in a more controlled phase), a growing scenario of budget cuts to science and education and denialism. Thanks to the scientific community, we could get vaccines, press the authorities to maintain the financial support (part of it at least, continuously) and can fight against misleading information. We are going down a dreadful path, and I sincerely and profoundly hope that we can overcome this. We as a nation, we as humanity. My deep gratitude to the scientific community.

Excuse me to write it in Portuguese:

Eu gostaria de agradecer a todos (as/es) e a tudo que direta ou indiretamente me influenciou e me ajudou a completar meu doutorado: família, amigos, professores, professoras, namorado, colegas, colaboradores, pessoas que me inspiram, o instituto, a biblioteca do instituto e as bibliotecárias, a universidade, as agências de fomento, a dança e as artes em geral... Em especial, eu gostaria de agradecer ao meu orientador, que possui um conhecimento imenso e que me oferece muito apoio e suporte. E mais: revisa o seu trabalho tão rápido e logo quanto alguém possa imaginar. Muito obrigada! Além disso, gostaria de agradecer à Thaty, que foi a primeira a me orientar e acreditar em mim, e que me ensinou praticamente tudo, e à Andressa, quem começou os estudos com a classe de quitosanas que usei neste trabalho, e me ajudou imensamente! Acima de tudo, eu gostaria de agradecer à ciência, e, ademais, os (as/es) cientistas, especialmente os brasileiros (as/es). Graças à comunidade científica, nós obtivemos vacinas, pudemos pressionar as autoridades para a manutenção do financiamento público (parte dele pelo menos, continuamente) e podemos lutar contra informações falsas e enganosas. Estamos percorrendo um caminho tenebroso, e eu sincera e profundamente espero que nós consigamos contornar isso. Nós como nação, nós como humanidade. Meu profundo agradecimento à comunidade científica.

This study was financed in part by the Coordenação de Aperfeiçoamento de Pessoal de Nível Superior - Brasil (CAPES) - Finance Code 001.

ABSTRACT

JOCHELAVICIUS, K. **Effects caused by water-soluble chitosans with high molecular weight in bacterial and mammal membrane models using Langmuir monolayers**. 2022. 62 p. Thesis (Doctor in Science) - Instituto de Física de São Carlos, Universidade de São Paulo, São Carlos, 2022.

Lipid monolayers are well-known systems that mimic cell membrane environments, being used in a variety of studies involving molecules that affect the membrane structure. Incorporation of chitosans into lipid monolayers is known to cause expansion and, mostly, fluidization, having stronger effects on negatively charged monolayers and with low molecular weight chitosans. These effects are attributed to a combination of electrostatic and hydrophobic interactions, correlating well with the stronger interactions with the negatively charged bacterial cell membranes than for mammalian membranes. In this thesis, we shall present results that challenge these interpretations. First, we employ water-soluble chitosans that induce larger effects on zwitterionic phospholipids, namely dipalmitoyl phosphatidyl ethalonamine (DPPE) and dipalmitoyl phosphatidyl choline (DPPC), than on negatively charged dipalmitoyl phosphatidyl glycerol (DPPG). Slightly stronger effects are induced on the lipid extract of *Escherichia coli* (*E. coli*), except when compared to DPPE on acetate buffer. Even more relevant is the effect induced on monolayers prepared with a ternary mixture of DPPC, cholesterol (Chol) and sphingomyelin (SM) (SM-DPPC-Chol), which represents lipid rafts, for which effects appear at chitosan concentrations that are orders of magnitude smaller than reported in the literature for other chitosans or types of monolayer. The differences from the literature may be attributed to the high acetylation degree of one of the chitosans used, named Ch35% as it has a 35% acetylation degree. The charge in Ch35% was not sufficient for the electrostatic interactions to predominate over the hydrophobic interactions. The importance of charge availability for such interactions was confirmed by the larger monolayer expansion induced by Ch15%, a chitosan with 15% acetylation degree. Because both chitosans were water soluble, experiments could be made with subphases at physiological pH and at an acidic pH. Ch35% tend to have larger effects on monolayers deposited on the acidic pH, with a few exceptions when the larger volume occupied by the chitosan at a high pH led to larges expansions. Surprisingly, Ch15% induced larger effects on physiologic pH when incorporated in *E. coli* lipids, and this remains an open point. Also worth mentioning is that Ch35% and Ch15% have high molecular weights, ca. 10^6 g mol^{-1}, and still produced stronger effects than low molecular weight chitosans in previous studies, again contradicting expectations from the

literature. In one hand, the larger effects induced on lipid rafts than on *E. coli* lipid extract calls for caution in the possible use of chitosans as bactericide agent; on the other hand, we observed a significant effect of Ch35% on monolayers of lipopolysaccharides (LPS), which represent the external wall of Gram-negative bacteria. Taken together, the results presented here indicate that charge availability and distribution in chitosans are probably the most important factor for their interaction with Langmuir monolayers, and the findings related to physiological pH and lipid rafts require a thorough revisit of studies on cell membrane models.

Keywords: Langmuir monolayers. Chitosan. Bactericide activity.

RESUMO

JOCHELAVICIUS, K. **Efeitos causados por quitosanas solúveis em água e de alta massa molar em modelos de membrana de mamíferos e bactérias, usando monocamadas de Langmuir**. 2022. 62p. Tese (Doutorado em Ciências) - Instituto de Física de São Carlos, Universidade de São Paulo, São Carlos, 2022.

Monocamadas lipídicas são sistemas conhecidos por mimetizarem membranas celulares, sendo usadas em uma variedade de estudos envolvendo moléculas que afetam a estrutura da membrana. Sabe-se que a incorporação de quitosanas em monocamadas lipídicas causa expansão e, em sua maioria, fluidização, com efeitos mais fortes em monocamadas carregadas negativamente e com quitosanas de baixa massa molar. Esses efeitos são atribuídos a interações eletrostáticas e hidrofóbicas, correlacionando bem com interações mais fortes com a parede celular negativa de bactérias do que com membranas de mamíferos. Nesta tese, apresentaremos resultados que desafiam essas interpretações. Primeiramente, empregamos quitosanas solúveis em água que induzem efeitos maiores nos fosfolipídios zwiteriônicos dipalmitoil etanolamina (DPPE) e dipalmitoil fosfatidilcolina (DPPC) do que no aniônico dipalmitoil fosfatidilglicerol (DPPG). Efeitos levemente maiores são induzidos no extrato lipídico de *E. coli*, exceto quando comparado com DPPE em tampão acetato. Mais relevante ainda é o efeito induzido em monocamadas compostas pela mistura ternária de DPPC, colesterol (Chol) e esfingomielina (SM) (SM-DPPC-Chol), que representa as jangadas lipídicas, para as quais aparecem efeitos com concentrações de quitosana que são ordens de magnitude do que reportado na literatura para outras quitosanas ou outros tipos de monocamada. As diferenças com a literatura podem ser atribuídas ao alto grau de acetilação de uma das quitosanas usadas, chamada de Ch35% por ter um grau de acetilação de 35%. A carga da Ch35% não foi suficiente para interações eletrostáticas predominarem sobre as hidrofóbicas. A importância da disponibilidade e da disposição de cargas para tais interações foi confirmada pela maior expansão das monocamadas induzida pela Ch15%, uma quitosana com grau de acetilação de 15%. Como ambas as quitosanas são solúveis em água, os experimentos puderam ser feitos em pHs fisiológico e ácido. A Ch35% tende a produzir efeitos maiores em monocamadas depositadas em pH ácido, salvas algumas exceções quando o volume ocupado pela quitosana em um pH alto levou a expansões maiores. Surpreendentemente, a Ch15% induziu efeitos maiores em pH fisiológico quando com lipídios de *E. coli*, e esse ponto ainda está em aberto. Mencione-se que a Ch35% e a Ch15% têm alta massa molar, cerca de 10^6 g mol^{-1}, e ainda produzem efeitos maiores em que quitosanas de baixa massa molar em estudos anteriores, novamente contradizendo

expectativas da literatura. Por um lado, os efeitos induzidos em jangadas lipídicas maiores do que no extrato de *E. coli* sugerem cautela no uso de quitosanas como agentes bactericidas; por outro, um efeito significativo foi observado em monocamadas de lipopolissacarídeos (LPS), que representam a membrana externa de bactérias Gram-negativas. Somados, os resultados apresentados aqui indicam que a disponibilidade e a disposição de cargas nas quitosanas são provavelmente o aspecto mais importante para a sua interação em monocamadas de Langmuir, e as descobertas relacionadas ao pH fisiológico e às jangadas lipídicas apontam para a necessidade de uma detalhada reanálise dos estudos em membranas celulares.

Palavras-chave: Monocamadas de Langmuir. Quitosana. Atividade bactericida.

LIST OF FIGURES

LIST OF TABLES

LIST OF ABREVIATIONS AND ACRONYMS

BLM	Bilayer or black lipid membranes
Chol	Cholesterol
Đ	Dispersity
DA	Degree of acetylation
DPPC	1,2-dipalmitoyl-sn-glycero-3-phosphocholine
DPPE	1,2-dipalmitoyl-sn-glycero-3-phosphoethanolamine
DPPG	1,2-dipalmitoyl-sn-glycero-3-phospho-(1'-rac-glycerol)
G	Gas
GlcN	Glucosamine
GlcNAc	N-acetylglucosamine
L	Liquid
LPS	Lipopolysaccharide
LC	Liquid-condensed
LE	Liquid-expanded
MD	Molecular dynamic
MW	Molecular weight
PBS	Phosphate-buffered saline
PC	Phosphatidyl choline
PE	Phosphatidyl ethalonamine
PG	Phosphatidyl glycerol
PM-IRRAS	Polarization-modulation infrared reflection absorption spectroscopy
S	Solid
SFG	Sum-frequency generation spectroscopy
SLB	Supported lipid bilayers
SM	Sphingomyelin

CONTENTS

1 INTRODUCTION

Biomembranes have the important role of holding the cellular material, acting as semi-permeable barriers that allow exchanges between intra and extracellular media. Since they participate in various biological events, exploring their features is a matter of interest. (1) Cell membranes have very complex structure and dynamics, which is why they are normally simulated with mimetic models to study their interactions, especially in order to obtain molecular-level information. (2-3) Membrane mimetic chemistry refers to organized surfactant assemblies and molecular hosts. The said assemblies include aqueous and reversed micelles, microemulsions, monolayers, organized multilayers, bilayer or black lipid membranes (BLMs) and vesicles. Molecular hosts include cyclodextrins (natural) and cavitands (synthetic), which are crown ethers, cryptands, and spherands. (4) With these models, it is possible to reproduce the structure of a membrane in a simplified way, and look closely to what happens in that environment. Furthermore, one is able to narrow down the number of variables involved in the experiment, particularly if the kind of answer desired is specified. The different models have comparative advantages and disadvantages; so often more than one mimetic system is used to study the same kind of event: their outcomes are complementary to each other. Besides experimental models, one may also resort to computational simulations. Molecular dynamic (MD) simulations are the most used, and becoming increasingly popular as computational processing capacity increases. They can provide atomistic-level detail, which cannot be acquired with experimental techniques, and can offer a rationalization of experimental results and provide predictions. (5–7)

In this PhD thesis, we use lipid monolayers as a mimetic system to investigate interactions with chitosans with well-controlled properties. Studying these interactions helps in describing the antimicrobial activity of chitosans. It is accepted that chitosan disrupts the bacterial membrane because of its NH_3^+ groups. The cationic group has the ability to interact with negatively charged components of the bacterial cell wall, such as lipids phosphate and carboxyl groups, N-acetylglucosamine and N-acetylmuramic acid, constituents of peptidoglycan. (8-9) This is indicated as the reason for the selectivity of chitosans over bacteria, relative to mammal cells. Experiments here are performed with neat phospholipids and mixtures that may be a more approximate model for the membrane. Bacterial and mammal membrane models are employed, and a homogenous N-acetylated chitosan, soluble in physiological pH. (10) In special, we chose the total lipid extract of *Escherichia coli* to represent a bacterium membrane for being a natural extract and having the composition of a model Gram-negative

bacterial membrane. Additionally, we also consider essential to measure the interaction with components of the bacterial outer membrane, so we also employed the lipopolysaccharide (LPS) from *E. coli* outer membrane.

In the literature of chitosans in Langmuir monolayers, we used to only find models composed by neat lipids, for mammal membranes or the inner bacterial membranes only. However, in a recent report, the lipid mixture employed presented surprising effects. (11) This mixture is known to form lipid rafts, which are domains commonly found in eukaryotic membranes, and chitosans affected its monolayers at much smaller concentrations than in previous studies. A recently synthesized chitosan, by Fiamingo *et al*. (10), and a commercial chitosan were used, and both produced effects at specially small concentrations, but the former was the most surprising. With these results, the models chosen until then to represent mammal membranes seemed to be limited, and they may not completely elucidate the factors responsible for chitosan effects on cell membranes. Furthermore, this new chitosan (called here Ch35%) is soluble in a wide range of pH, unlike previously used chitosans that are only soluble in acidic pH. Considering the enhanced effect and the solubility, we decided to investigate the use of this chitosan –and, later, a chitosan also synthesized by Fiamingo *et al*. (10) with a lower degree of acetylation (DA)– in bacterial membrane models.

We investigated the interaction of two chitosans with DAs of 35% (Ch35%) and 15% (Ch15%) with different lipids and a lipid extract, from the inner membrane, and a LPS, from the outer membrane. The lipids and the LPS used were: dipalmitoyl phosphatidyl choline (DPPC), dipalmitoyl phosphatidyl ethalonamine (DPPE), dipalmitoyl phosphatidyl glycerol (DPPG), total lipid extract from the bacterium *E. coli* and LPS from *E. coli* (J5, Rc mutant) The pressure-area isotherms were compared with DPPC and a mixture containing DPPC, sphingomyelin (SM) and cholesterol (DPPC-SM-chol (1:1:1)), studied by Pereira and co-workers. (11) The zwitterionic phospholipids DPPC and DPPE, and the anionic DPPG have all the same hydrocarbon tails, but different headgroups. Phosphatidyl glycerol (PG) and phosphatidyl ethalonamine (PE) are both typically present in bacterial membranes (12), while phosphatidyl choline (PC) is typical of mammalian cell membranes, mostly present in the outer leaflet. The latter also have PE in their composition, mostly in the inner leaflet. (13)

A relevant contribution in this study lies in the use of high molecular weight chitosans soluble at physiological conditions, synthesized by Fiamingo and co-workers. (10) Commercially available chitosans with similar molecular weight are only soluble at acidic pH, which hampers their study under different conditions. Though water-soluble chitosans have been reported in other works in the literature, they have low molecular weight due to

depolymerization. We aimed to characterize the interaction of Ch35% and Ch15% with lipid films at the physiological pH of 7.4. In addition, to contrast the results with the existing literature, we also studied film properties at pH 4.5.

2 LITERATURE REVIEW

Biological membranes protect and separate the content of a cell from the external medium. They participate in cellular processes for maintaining the morphology, cytoskeletal dynamics and asymmetric distribution of membrane lipids. In addition, membranes take part in homeostasis by responding to stimuli and intermediating the passage of solutes and molecules between the internal and external media. (1) The first model to describe biomembranes satisfactorily was presented by Singer and Nicolson, who suggested the mosaic-fluid model in 1972. (14) This model is still relevant and accurate, particularly after it was revised with information accumulated since the 1970s. It describes the membrane as a matrix formed by a fluid phospholipid bilayer, intercalated with mobile globular proteins and glycoproteins. In the most recent version of the model, also considered is the interaction with the extracellular matrix and the possibility of domain formation. These domains would be islands with less mobility in a sea of fluid phospholipids. Molecules are assembled as "non-uniform, non-random cooperative elements in thermodynamic equilibrium phases with compositional fluctuations." (15)

To study events at the membrane level, researchers have developed mimetic systems to simplify the analysis, reproducing only the environment that is relevant for the object of study. Supported lipid bilayers (SLBs), unilamellar vesicles of different sizes, bilayers or black lipid membranes (BLMs) and lipid monolayers are examples of model membranes. (1-4,16) Lipid monolayers, for being one layer of lipids, as the name suggests, model half of a membrane. They are ideal to assess events that take place at the membrane in two dimensions. The advantages of this model include the possibility to change lipid composition and density. (4,17-18) Furthermore, the experiments are conducted in an aqueous medium, which is biologically relevant. The physicochemical properties such as surface pressure, temperature, subphase composition, pH and the area available for each molecule, can be controlled. Another advantage of monolayers is that only small amounts of reagents and molecules are necessary for the experiments. (19) Obviously, using monolayers is disadvantageous when phenomena such as transport across the membrane are to be studied.

The monolayer technique is useful to investigate the action of drugs, peptides and proteins in the membrane as well as of many other biologically-relevant molecules and nanomaterials. (20) For instance, Langmuir monolayers were applied to evaluate the interaction between cell membranes and various pharmaceutical drugs and potential pharmaceutical drugs, such as curcumin (21), paclitaxel (22), local anesthetics (23) and nitrofurantoin. (24), as well

as nanoparticles for drug delivery. (25) Also, there are many studies with proteins, peptides and enzymes, like the fungal phospholipase *Lecitase ultra* (26), the Dengue fusion peptide (FLAg) (27), the α-lactalbumin (forming an antitumoricidal lipid−protein complex). (28) It is also possible to find the combination of more than one of these molecules affecting Langmuir monolayers, as penicillin-binding proteins (PBPs) and the antibiotics meropenem and methicillin. (29)

One of these molecules is chitosan, a chitin derivative, which is the most abundant polysaccharide in Nature after cellulose. Chitin can be obtained from crab, shrimp, krill shells and fungi. (9-10) Naturally-occurring polysaccharides have potential application in biomedicine owing to their biocompatibility, biodegradability and non-immunogenicity. Chitosan can be applied in food, pharmaceutical and cosmetics industries, medicine, biotechnology, agriculture and water treatment. (9) The degree of acetylation (DA), molecular weight (MW) and dispersity – which reflects the broadness of the MW distribution – determine the physicochemical properties of chitosans. (10) Depending on these properties and characteristics of the aqueous medium, their dispersion varies, and so does their conformation. (30-31)

A glucosaminoglycan polymer featuring β (1→4)-linked glucosamine (GlcN) and N-acetylglucosamine (GlcNAc) units, chitosan derives from the partial *N*-deacetylation of chitin. Its structure is illustrated in Figure 1. Most chitosans have more GlcN than GlcNAc units (DA < 50%) and are soluble in dilute acid solutions, which enable the protonation of the amino groups. (9-10) The chitosans used in this work, named Ch35% and Ch15%, were synthesized by Fiamingo *et al*. (10), and have DAs of 35% and 15%, i.e., 65% and 85%, respectively, of GlcN units, randomly distributed. This random distribution, not encountered in commercially available chitosans, allowed for solubility of high molecular weight chitosans even in phosphate-buffered saline (PBS) pH 7.4, mimicking physiological conditions. (10)

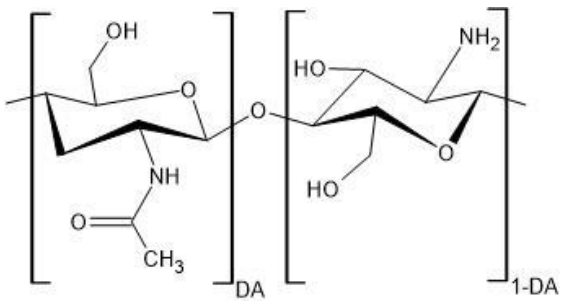

Figure 1 - Chitosan basic structure, characterized by the degree of acetylation (DA).
Source: By the author

The literature on chitosan is vast (9,32–38), including works on interaction with lipid monolayers. (39–45) Even though most of the biological relevant media has a pH close to 7, the first studies with chitosans at pH 7.4 (pH of human body fluids) were published only in 2020. De Oliveira Pedro *et al*. (44) used low molecular weight and chemically-modified chitosans, and Pereira *et al.* (11) used the same high molecular weight Ch35% as here. Earlier studies were all conducted in acidic media. In most studies, the incorporation of chitosan causes expansion of the films and decrease in compressional modulus. (20)

Polarization-modulation infrared reflection absorption spectroscopy (PM-IRRAS) measurements on monolayers containing DMPA, DPPC and DPPG showed that incorporation of chitosan changed the spectra on polar and hydrophobic regions. This suggests that chitosan interacts with both the lipids headgroups and the hydrocarbon tails through electrostatic and non-electrostatic forces. (46–48) Even though DMPA and DPPG are anionic, opposite effects were observed regarding their acyl chains ordering. For the first, there was an increase in order, while a decrease in order was observed for DPPG. These conclusions were based on experiments with PM-IRRAS and sum-frequency generation spectroscopy (SFG). (46,48,49) The chitosans used in the studies above were either commercially acquired (DA = 22%, $\overline{MW}$ = 4.79× 10^5 g mol^{-1}, Đ = 4.2) (46,48), or synthesized by the authors in those references: one with DA = 10%, $\overline{MW}$ = 2.35 × 10^3 g mol^{-1} (considered a low MW) and Đ = 2.7 (46); two with DA = 6% (one with high molecular weight: $\overline{MW}$ = 730,000 g mol^{-1} and Đ = 2.6, one with low molecular weight: MW = 8.8 × 10^3 g mol^{-1} and Đ =2.8) (47), and another with DA = 15%, $\overline{Mn}$ = 1.087 × 10^5 g mol^{-1} (which is the number average MW, smaller than the mass average MW ($\overline{MW}$)) and Đ = 6.2. (49)

In addition to how the incorporation of chitosan affected the monolayers, they also verified that the low molecular weight chitosans caused a greater effect on the monolayers. This was associated with the smaller size, which would facilitate chitosan penetration in the films. (46-47) In ref. (47), the authors also suggested that this conclusion might be biased since the chitosans had the same DA and similar dispersity. However, the waiting time before compression was fixed, and so it was possible that adsorption was not saturated for all samples. In ref (46), the DAs were disparate (10% for low molecular weight and 22% for high molecular weight chitosans) and the dispersities were also different (2.7 and 4.2, respectively). Despite such differences, it appears to be a trend that smaller chitosan molecules cause a stronger effect on lipid monolayers. In ref. (46) there was also a comparison of results from refs (49) and (50), from which it was concluded that chitosans with higher DA induce a larger area expansion in

the isotherms containing DMPA molecules. The interpretation was that the acetyl groups were important for their taking part in hydrophobic interactions.

Another group of scientists studied the thermodynamics of the interactions between chitosan and DPPG or DPPC, at different pH values and temperatures. They also concluded that electrostatic and non-electrostatic forces are present, but the latter are the main cause of the effects on the monolayer properties assessed: lift-off area, limiting area, compressional modulus, and parameters describing the transition from liquid-expanded to liquid-condensed phase. (51–53) The chitosan used had DA = 17%, and the viscosity-average molecular weight of this chitosan was Mv = 1.202×10^6 g mol^{-1}. In all the studies mentioned, the incorporation of chitosan was found to cause a stronger effect on negatively charged lipids, and this was related to its polycationic character. (46,48-49,51-52)

The effect of chitosan was also assessed on monolayers containing cholesterol and fatty acids. In all cases, chitosan expanded the monolayers and did not cause a change in the phase state, but reduced the compressional modulus of cholesterol, making the monolayers more compressible. (40,48,51,53) For fatty acids, the effect was similar, although it yielded an increase in the compressional modulus for unsaturated acids. (40) In ref. (40), they used a chitosan with DA = 30% $\overline{MW}$ = 3.3×10^5 g mol^{-1}. As already mentioned, in ref. (48) the chitosan had DA = 22% and $\overline{MW}$ = 4.79×10^5 g mol^{-1}, whereas in ref. (51) DA = 17% and Mv = 1.202×10^6 g mol^{-1}. In ref. (53), three chitosans were used: one with DA = 19% and Mv = 360×10^3 g mol^{-1}, the other as in ref. (51), and the third with DA = 23% and Mv = 2.506×10^6 g mol^{-1}. In the latter, they also concluded that smaller (low MW) chitosans cause a stronger disturbance in the monolayers (containing either DPPC, DPPG or cholesterol), especially when formed by cholesterol. They associate this finding with higher mobility of shorter polymers.

Only in 2022 could we find a study on the effect of chitosan incorporation onto an unsaturated phospholipid monolayer, containing DOPC. (54) When 0.1 mg mL^{-1} of chitosan was added to the subphase containing water with acetic acid 0.1% (used to solubilize the chitosan), it caused monolayer expansion, though small. The compressional modulus did not change considerably. This differs for the fatty acids, as described, but perhaps a higher chitosan concentration could promote more visible changes. Another question is the 10 min waiting time before compression, which might not be enough for chitosan adsorption (in comparison with 20 min in the study with fatty acids). In another study from the same group, they also used DOPC and chitosan with other substances, under the same conditions. (55) However, the values of the lift-off areas (A_0), the difference between the lift-off areas with and without chitosan in the subphase (ΔA_0) and the maximum compressional moduli presented in each work were a

little different from each other. These differences are small, but so are the area expansions (ΔA_0 = 3.6 Å and ΔA_0 = 4.2 Å, respectively). The compressional moduli are approximately equal for the isotherms with and without chitosan in the same work, but there is a difference of an order of 10 mN m^{-1}, from one to another. Comparing with a previous work of the same group (56), in which they used a DPPC – saturated, analogous to DOPC – monolayer with the same conditions as well, the effect was similar. However, there is a region in which the compressional modulus of DPPC monolayer in pure water or in water with acetic acid only, decreases, and it increases again later. This happens between 20 and 30 mN m^{-1}, and so the compressional modulus in the presence of chitosan becomes higher than without it at about 23 to 35 mN m^{-1}. That does not happen with the DOPC film. The chitosan used in these studies had a DA of 18% and MW ranging from 1.0 to 3.0 × 10^5 g mol^{-1}.

The first study with Ch35% (11) showed an enhanced effect on monolayers containing a lipid mixture of SM-DPPC-Chol (1:1:1), compared to the effects of other chitosans and on neat DPPC monolayers. This mixture forms lipid rafts, microdomains that are common in eukaryotic cells. That is to say, this model system is more realistic than neat DPPC. The incorporation of Ch35% caused monolayer expansion, with a stronger effect at pH 4.5 than at pH 7.4. At the latter pH, the compressional modulus decreased when a small amount of Ch35% was present in the subphase (10^{-4} mg mL^{-1}), but for higher amounts (10^{-3}, 10^{-2} and 10^{-1} mg mL^{-1}), it increased. On acidic pH, there was monolayer expansion for Ch35% concentration as low as 10^{-6} mg mL^{-1}, and apparently saturated the monolayer, since no significant expansion was observed for higher concentrations. The compressional modulus was also increased, which indicates a higher rigidity of the films. At the molecular-level, PM-IRRAS spectra presented shifts and appearance of bands in the non-polar and polar regions, which proves that incorporation of Ch35% modified the organization and orientation of the lipids headgroups and hydrocarbon tails. It is also relevant that most of the works in the literature use chitosan at a concentration range from 0.02 to 0.3 mg mL^{-1} (39,46–48,54,56), and even 1 mg mL^{-1}. (51–53) The ideal amount of chitosan for each monolayer –and, consequently, for each of its applications– depends on its properties, as well as characteristics of the media.

In summary, the interactions of chitosan in lipid monolayers cause expansion and change the organization and the orientation of film molecules. The extent of these modifications, as well as the minimum concentration necessary to produce detectable changes and the nature of the chemical interactions, will depend on the film composition, on the subphase and characteristics of chitosan such as DA, pattern of acetylation (PA), MW and dispersity (Đ, formerly the polydispersity index (PDI)).

3 MATERIAL AND METHODS

3.1 MATERIALS

The phospholipids DPPC (1,2-dipalmitoyl-sn-glycero-3-phosphocholine), DPPE (1,2-dipalmitoyl-sn-glycero-3-phosphoethanolamine), DPPG (1,2-dipalmitoyl-sn-glycero-3-phospho-(1'-rac-glycerol) and *E. coli* total lipid extract, represented in Figure 2, were purchased from Avanti Polar Lipids Inc. As informed in the manufacturer's website, the *E. coli* extract contains 57.5% in mass of L-α-phosphatidylethanolamine (PE), 15.1% of L-α-phosphatidylglycerol (PG), 9.8% of cardiolipin (CL) and 17.6% of unknown components. Because of these unknown components, the molecular weight is not determined, and the isotherms are expressed in area per lipid mass instead of mean molecular area. Lipopolysaccharides (rough strains) from *Escherichia coli* J5 (Rc mutant) were purchased from Sigma-Aldrich. Since there is no information about its molecular weight, their π-A isotherms were also plotted as a function of area per lipid mass. NaCl, KCl, Na_2HPO_4, KH_2PO_4, $C_2H_3NaO_2$ (P.A. grade), glacial acetic acid –for buffer preparation–, chloroform (HPLC grade) and methanol– for lipid solubilization– were purchased from Panreac, Sigma-Aldrich, J.T.Baker, Synth and Qhemis, respectively.

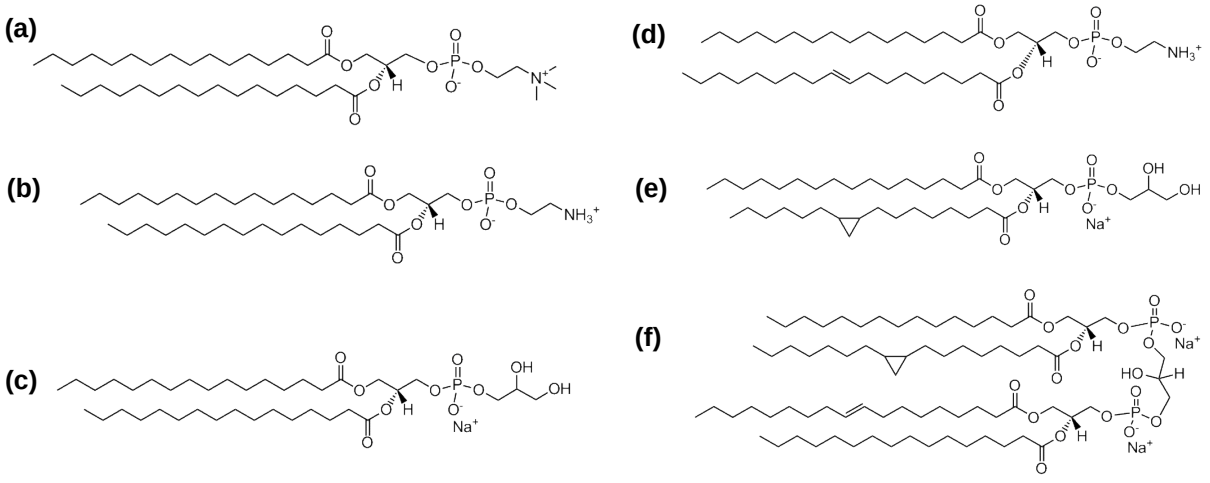

Figure 2 - Structure of the phospholipids: (a) DPPC, (b) DPPE, (c) DPPG, (d) *E. coli* PE (one possible structure), (e) *E. coli* PG (one possible structure) and (f) *E. coli* CL (one possible structure).
Source: PHOSPHOLIPIDS (57)

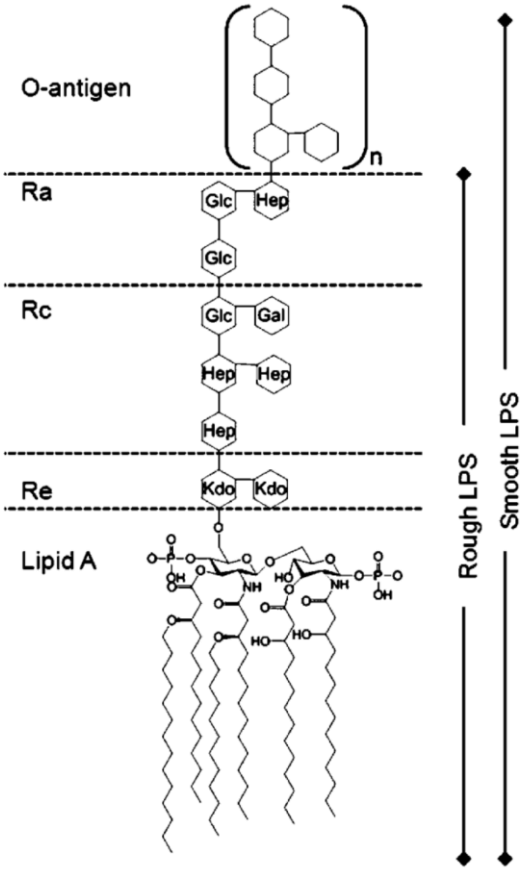

Figure 3 - Schematic representation of *E. coli* LPS, from rough and smooth strains. Gal: galactose; Glc: glucose; Hep: L-gycero-D-manno heptose; Kdo: 2-keto-3-deoxyoctonoic acid.
Source: LE BRUN. (58)

DPPC and DPPE are zwitterionic phospholipids, while DPPG is anionic, all having saturated acyl chains bearing 16 carbons. The *E. coli* extract is a mixture of various kinds of lipids: charged, uncharged, polar, non-polar, containing acyl chains with different lengths and saturation degrees. The DPPC headgroup has three methyl groups bonded to the nitrogen atom (a choline group), while DPPE has three hydrogen atoms (an amino group). Gram-negative bacteria contain an outer membrane, which is a bilayer comprising phospholipis in its inner leaflet, and LPSs in its outer leaflet. The latter are formed by lipid A and a polysacharide core –in rough mutants–, and, additionally, O-antigen –in smooth strains. (58) A representation of LPS structure is given in Figure 3.

The chitosans studied here, namely Ch35% and Ch15%, were obtained by Dr. Anderson Fiamingo using a multistep ultrasound-assisted deacetylation process (USAD process), as described in ref. (10) Three rounds of USAD were conducted, and a subsequent partial N-acetylation was performed to obtain chitosans with varied DAs. Fiamingo used mild conditions to avoid depolymerization and obtain a predominantely random distribution of GlcN and GlNAc units. These chitosans present high weight average molecular weight ($\overline{MW} \approx 1 \times 10^6$ g

mol^{-1}), high weight average degree of polymerization ($\overline{DP_W} \approx 6000$) and quasi-ideal random distribution of GlcN and GlcNAc units (PA ≈ 1.0). Specifically, Ch35% has DA ≈ 35%, molecular weight ($\overline{MW} = 1.05 \times 10^6$ g mol^{-1}) and a PA of 1.00. Ch15% has DA ≈ 15.5%, similar molecular weight ($\overline{MW} = 0.99 \times 10^6$ g mol^{-1}) and a PA of 1.03. (10) The pK_a of the amino group of the chitosans is ≈ 6.5 (9), but it varies depending on DA, Mw and ionic strength of the media. The buffers we used have pH 4.5 and ionic strength of 0.05 M, and pH = 7.4 and ionic strength of 0.1 M. In a study with a chitosan of Mw around 369 000 g mol^{-1}, with varying conditions, a chitosan with DA = 35.1% presented $pK_a \approx 6.8$ at pH = 4.5 and ionic strength of 0.05 M, and $pK_a \approx 6.7$ at pH = 7.4 and ionic strength of 0.1 M. A chitosan with DA = 15.8% had $pK_a \approx 6.0$ at pH = 4.5 and ionic strength 0.1 M (there was no data available for 0.05 M), and $pK_a \approx 6.4$ at pH = 7.4 and ionic strength 0.1 M. (31)

3.2 LANGMUIR FILMS

Lipids are amphiphilic molecules with the ability of forming monomolecular films at the gas-liquid interface, which are referred to as Langmuir films or monolayers. Using a Langmuir trough, it is possible to measure the surface pressure (π), defined as the difference between the surface tension of the liquid surface without (γ_0) and with the film deposited (γ) (59):

$$\pi = \gamma_0 - \gamma \qquad (1)$$

The surface pressure is measured using the Wilhelmy plate method, in which an electrobalance measures the force due to the surface tension exerted on a plate made of platinum, glass, mica, quartz or filter paper. The dimensions of the plate and the contact angle with the liquid over which the surface tension is measured are depicted in Figure 4. The plate is subjected to the following forces: weight (W) and surface tension (γ) pointing downward (if the meniscus is downward, as in the scheme) and buoyancy (ξ) pointing upward, whose resultant is given in equation 2. We can write each of them in terms of the gravity acceleration (g), the dimensions presented in Figure 4, the densities of the plate (ρ) and the water (ρ_w) and the water surface tension (γ_w), as shown in equations 3, 4 and 5. Finally, we obtain equation 6.

$$F = W + \gamma - \xi \qquad (2)$$

$$W = \rho glwt \quad (3)$$

$$\gamma = 2(w + t)cos\theta\gamma_w \quad (4)$$

$$\xi = hwt\rho_w g \quad (5)$$

$$F = \rho glwt + 2(w + t)cos\theta\gamma_w - hwt\rho_w g \quad (6)$$

If the plate is completely wetted by the liquid, θ = 0, therefore $\cos\theta = 1$. The plate thickness is negligible, compared to the other values, so that the perimeter can be approximated to 2w. Considering the system in stationary equilibrium, the weight (W) and the buoyancy (ξ) are constant. Thus, using equations 1 and 6, we obtain the surface pressure in terms of the force over the plate (62-63):

$$\pi = -\Delta\gamma = -\Delta F/2w \quad (7)$$

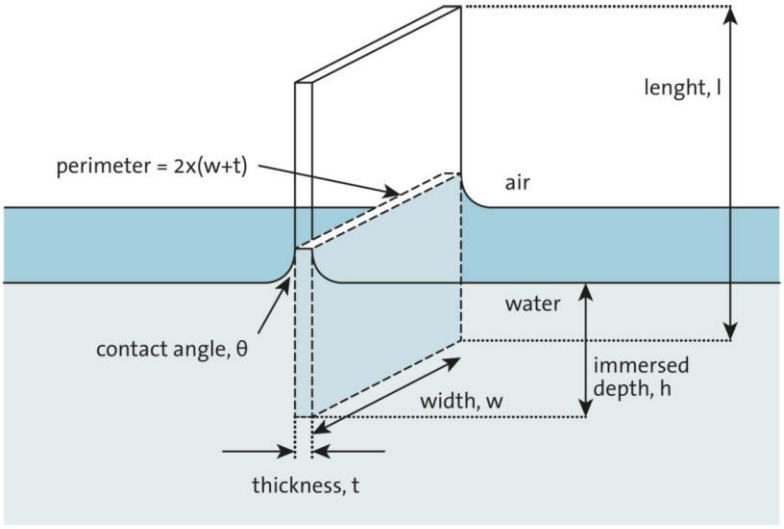

Figure 4 - Wilhelmy plate partially submerged in water
Source: KSV NIMA. (60)

Pressure-area (π-A) curves depend on the temperature. They are therefore taken under constant temperature, being named surface pressure isotherms. Initially, with an area sufficiently large, the molecules of the amphiphile do not interact, being on the gas phase (G). As the area reduces, they start to interact and transition to the liquid (L) and, later, to the solid phase (S). With further compression, they achieve collapse, forming 3D structures. Some films do not achieve the solid phase before collapsing, depending on their packing capacity. In addition, the liquid phase can be split into liquid-expanded (LE) and liquid-condensed (LC) phases, and some monolayers exhibit a phase transition plateau. These phases and phase

transitions are better identified by the derivative of the surface pressure isotherms, relatively to the area occupied by the molecules. There is a quantity named compressional modulus defined by:

$$C_S^{-1} = -A\left(\frac{\partial \pi}{\partial A}\right)_T,$$

where A is the mean molecular area (or area per lipid mass), π is the surface tension and T the temperature. Since the latter is kept constant, we can also suppress it. This quantity is plotted as a function of the surface pressure or the molecular area, giving information about the elasticity of the film. This is why it is also called in-plane elasticity. The higher the value of the modulus, the greater the rigidity, and vice-versa. We can designate the two-dimensional phases of the monolayer according to the value of the compressional modulus, as follows: lower than 12 mN m^{-1} for gas, 12–100 mN m^{-1} for LE, 100–250 mN m^{-1} for LC and higher than 250 for solid (S). (61)

For the surface pressure measurements, we used homemade Langmuir troughs bearing a volume of 65 mL and a superficial area of 75 x 323 mm^2. They are coupled to the original KSV NIMA devices, either a KSV 5000 device or a more modern frame (standard size) with the surface pressure sensor and the interface unit common to all of their current troughs. The Wilhelmy plate used was made of filter paper, and there were two movable barriers that control the surface area to obtain π-A isotherms. These systems are placed in a class 10000 clean room, with temperature of 22 ± 1 ºC.

Phospholipids or LPS were solubilized at 0.5–1.0 mg mL^{-1} in chloroform, chloroform:methanol (4:1, v/v) for DPPG, or chloroform:methanol:water (60:39:1, v/v/v) for LPS, and spread onto the subphase using a microsyringe. We allowed 30 min for solvent evaporation and interaction between the molecules in the film and chitosan. The film was then compressed at a rate of 10 mm min^{-1}. The subphase consisted of 0.16 M phosphate-buffered saline (PBS) pH 7.4 – prepared according to Cold Spring Harbor Protocols (62) – or 0.05 M acetate buffer at pH 4.5. The latter was prepared with 0.02 M sodium acetate and 0.03 M glacial acetic acid. To the buffers, we added one of the chitosans (Ch35% or Ch15%) in different concentrations: 0, 10^{-5}, 10^{-3} and 10^{-1} mg mL^{-1}. Ultrapure water with resistivity of 18.2 MΩ cm was obtained from a Milli-Q system. We did not obtain π-A isotherms of the phospholipids in subphases containing Ch15%, neither did we obtain isotherms of the LPS in PBS with Ch15%. In order to solubilize in PBS, 20 mg of the dry samples of Ch35% or Ch15% were first dissolved

into 50 µL HCl diluted 10 × and a small amount of water (~50 mL). After stirring for ca. 24 h, this solution becomes homogenous, and we complete the volume with a solution of PBS concentrated 10× and water to obtain 10^{-1} mg mL^{-1} of Ch35%. To solubilize in acetate buffer, the dry samples are added directly into the buffer to stir (also for ~24h), at the final concentration. The lower concentrations are obtained diluting these stock solutions.

4 RESULTS AND DISCUSSION

The results presented in sections 4.1, 4.2 and 4.3 are already published in. (63) Results will be shown for isotherms containing DPPC, DPPE, DPPG and *E. coli* lipid extract, in subphases containing PBS or acetate buffer with different concentrations of Ch35%.

4.1 Zwitterionic phospholipids and Ch35%

We shall analyze isotherms of the phospholipids on pure buffers (with no chitosan). The first worth noting featuring is related to the isotherms of the zwitterionic lipids DPPC (Figure 5 and Figure 6) and DPPE (Figure 7), which are entirely different from each other, in spite of their similar molecular structures. These differences can be explained by the different volume occupied by their headgroups. Structural differences mentioned in section 3.1 confer a smaller volume to DPPE and the ability to form intermolecular hydrogen bonds when arranged in a Langmuir monolayer. (64-65) The first two large differences in their behaviors are the lift-off area and the phase transition. DPPE isotherm shows a much smaller lift-off area, being practically half of DPPC on a PBS subphase. Also, there is no plateau in the transition from liquid expanded (LE) to liquid condensed (LC) phases, unlike the case of DPPC. The packing capacity of DPPE molecules appears to be much higher. This is an effect not only of the electrostatic interactions between charged groups – as in the zwitterion in DPPC films – but also of the hydrogen bonds between the phosphate and amino groups. (64) The compressional moduli are considerably higher for DPPE at both pHs. In fact, at 30 mN m^{-1} DPPC (Figure 5 and Table 1) and DPPE (Figure 8 and Table 2) monolayers are in the LC phase. DPPE is practically in the solid phase on acetate buffer (Figure 8b and Table 2), when considering the values assigned for each phase, according to Section 3.2. At this pressure range, the lipid packing is similar to that on a biomembrane. (3) Despite the packing difference, affinity for Ch35% is only slightly different between DPPC and DPPE, as we shall see.

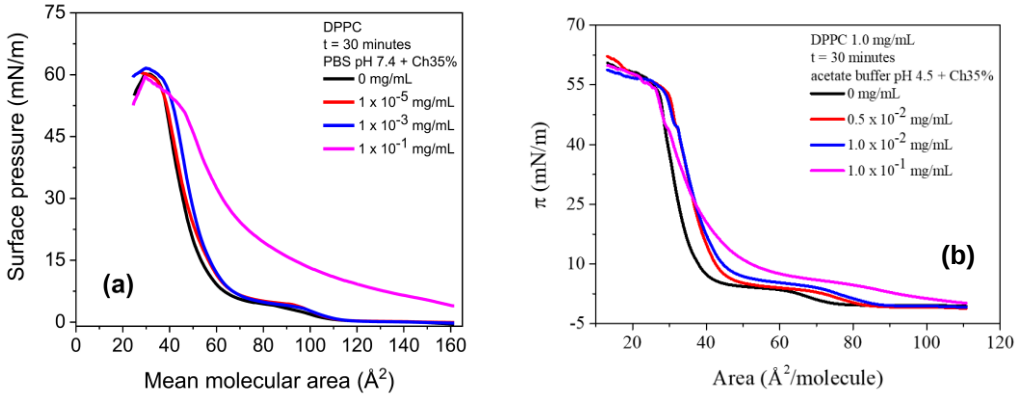

Figure 5 - Pressure-area isotherms of DPPC monolayers on PBS pH 7.4 (a) and acetate buffer pH 4.5 (b) containing different concentrations of Ch35%

Source: (a) JOCHELAVICIUS (63); (b) PEREIRA (11)

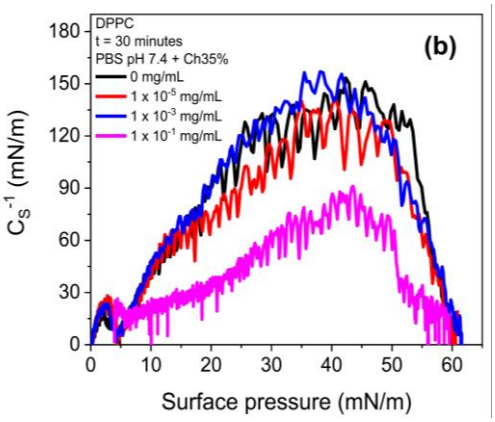

Figure 6 - Compressional moduli of DPPC π-A isotherms on PBS pH 7.4 containing different concentrations of Ch35%

Source: JOCHELAVICIUS (63)

Before discussing the modifications induced by chitosan, it should be mentioned that chitosan dissolved in the buffer does not present surface activity, i.e., it will not adsorb at the air/water interface in order to generate a surface pressure isotherm with significant pressure values. For DPPC on PBS in Figure 5, we noticed significant changes only at the highest Ch35% concentration tested (10^{-1} mg mL^{-1}), but a small expansion also appears at 10^{-3} mg mL^{-1}. Figure 6 shows the effects from Ch35% on DPPC monolayers on acetate buffer (pH = 4.5) obtained by Pereira *et al.* (11), which indicates a similar effect to that observed at pH 7.4, considering that chitosan concentrations used were slightly different. There seems to be a slightly stronger effect on acetate buffer, since there is already a significant shift at 0.5×10^{-2} mg mL^{-1} (5 × more concentrated than our intermediary concentration of 10^{-3} mg mL^{-1} on PBS). At the highest concentration, however, monolayer expansion was considerably higher on PBS, while the collapse pressure was lower. This effect could be related to the volume occupied by

chitosan in each medium. The chain organization of Ch35% depends on the pH, since the amino groups of GlcN units are prone to protonation. They are mostly converted to ammonium groups at pH ≤ 6.0. In acetate buffer, the positive charges suffer repulsion, and the intrachain hydrogen-bonds with carbonyl groups of GlcNAc units will confer rigidity and a more extended conformation to the polymer. This does not apply for pH 7.4. According to Flamingo and co-workers (10), the diameter measured for Ch35% on acetate buffer was 16.2 ± 1.7 nm, while on PBS the diameter was 26.7 ± 1.1 nm. A more bulky chitosan incorporated to the film should have caused a larger expansion and greater destabilization of the interactions among molecules in the film. At high surface pressures the increase in area on acetate buffer decreased, as if Ch35% was being expelled from the interface, back to the subphase.

Table 1 - Maximum and compressional modulus values at 30 mN m^{-1} of DPPC films on either PBS or acetate buffer pH 4.5 with different amounts of Ch35%

	C_S^{-1} at 30 mN m^{-1}		**C_S^{-1}, max**	
Concentration of Ch35%	**PBS**	**Acetate**	**PBS**	**Acetate**
0 mg mL^{-1}	125	168	152	186
10^{-5} mg mL^{-1}	106	NA	139	NA
10^{-3} mg mL^{-1}	126	163*	156	175*
10^{-1} mg mL^{-1}	57	84	90	110

*These values are for the concentration of 5×10^{-3} mg mL^{-1}

Source: JOCHELAVICIUS (63)

Figure 5b shows the compressional moduli curves, featuring a change in the DPPC monolayer organization when Ch35% was present on PBS. Ch35% induced a reduction in the modulus. This also occurred with the acetate buffer, according to the data provided by Dr. Andressa Pereira from ref. (11). The maximum and the values at 30 mN m^{-1} of compressional moduli, obtained here (on PBS) and provided by Dr. Pereira (on acetate buffer), are shown in Table 1. A reduction means that Ch35% made the monolayers less rigid. Most of the literature on interaction of chitosans with lipid monolayers shows that there is a decrease in the modulus. For DPPC, studies performed on Theorell-Stenhagen (TS) pH 3.0 and on 0.6 M acetate buffers with pHs 3.5, 4.75 and 6.0, all report a reduction. (46,51,53) These studies used chitosans with DA of 22% and 17± 5%, and molecular weights lower than the one used here. In contrast, films containing the mixture SM-DPPC-chol (1:1:1) on PBS had their compressional moduli increased for the lowest concentrations of Ch35% (10^{-5} and 10^{-4} mg mL^{-1}), which also happened in the work by Pereira et al. For higher concentrations, the modulus decreased. On

acetate buffer, however, the moduli were all higher than for the ternary mixture alone within the concentration range investigated. (11) Taken together these results indicate that – in contrast to previous results for neat phospholipids - the SM-DPPC-chol (1:1:1) monolayer became more rigid in the presence of chitosan.

For DPPE monolayers, Figure 7a shows that 10^{-3} mg mL^{-1} Ch35% on PBS already shifted the isotherm to higher molecular areas, but the shift for 10^{-1} mg mL^{-1} is more pronounced, similarly to DPPC. At lower surface pressures, the expansion of the DPPE monolayer was larger, and the pressure registered at the beginning was much higher than zero. This happened because we wanted to keep the initial area occupied by the molecules of the film the same for all experiments so that their quantity would be the same, and only the concentration of chitosan would change. Otherwise, the ratio of molecules in the film to chitosan molecules in the subphase would not change in the same proportion as the chitosan concentration. With increasing pressure, this expansion decreased faster than for DPPC. At higher pressures there is a plateau, and the isotherm encounters the one with 10^{-3} mg mL^{-1} of chitosan, keeping the same profile until collapse. This is an indicative that chitosan molecules were expelled from the films, and continue to interact only with the phospholipids headgroups through electrostatic interactions. From the compressional moduli in Figure 8a, one notes that the DPPE monolayer is in the LE phase in the presence of Ch35%. This is in contrast to a typical DPPE monolayer which is mostly liquid condensed (LC phase). The plateau, when the modulus approaches 0, determines the phase transition from LE to LC. As already mentioned, hydrogen bonds between DPPE molecules enable a close packing. Once these bonds break, the monolayer loses structure with the molecules moving away from each other. That is caused by the incorporation of chitosan in the film. The tight organization leaves no room for the polymer to penetrate; at high concentrations, it is able to destabilize this organization, and penetrates into the hydrocarbon tails.

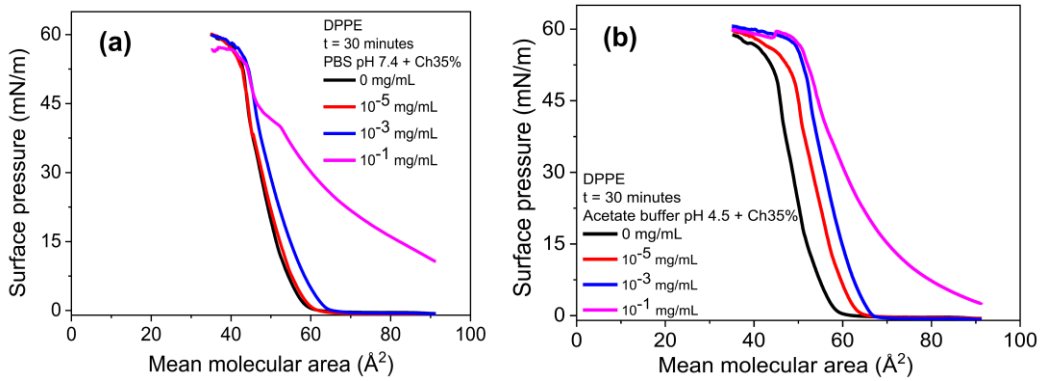

Figure 7 - Pressure-area isotherms of DPPE monolayers on PBS pH 7.4 (a) and acetate buffer pH 4.5 (b) containing different concentrations of Ch35%
Source: JOCHELAVICIUS (63)

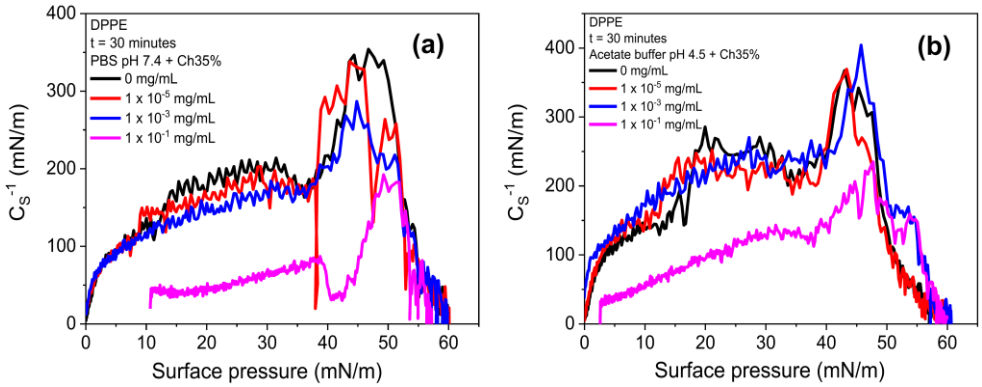

Figure 8 - Compressional moduli of DPPE π-A isotherms on PBS pH 7.4 (a) and acetate buffer (b) containing different concentrations of Ch35%
Source: JOCHELAVICIUS (63)

On acetate buffer, the DPPE monolayer expanded even for the lowest chitosan concentration of 10^{-5} g mL^{-1} (b). This trait is expected due to protonation of the amino groups on more acidic media (10), facilitating the interaction with phosphate groups in the lipid headgroups. The compressional modulus also decreased, which is evident for the highest chitosan concentration (10^{-1}mg mL^{-1}). In that concentration, the monolayer state was altered to an expanded one. Similarly to what happened on PBS, the decrease in modulus decreased with increasing pressure, and the monolayer returned to its condensed state. Collapse occurred at the same pressure and area as the isotherm for 10^{-3} g mL^{-1} Ch35%. This change of state, however, was not marked by a plateau. As the modulus of compressibility only changed significantly for the highest concentration of Ch35%, the monolayer organization was kept for the lower concentration, even though there was a significant expansion. This suggests that the Ch35% molecules intercalate with the lipid molecules but do not interfere with their intermolecular interactions. These interactions were only affected when 10^{-1}mg mL^{-1} of Ch35% was present in the subphase. In addition, the disturbance caused by Ch35% was greater

on PBS than on acetate buffer. That is a consequence of the larger volume occupied by Ch35% on PBS, as discussed for DPPC monolayers. Table 2 contains the values of the compressional moduli at 30 mN m^{-1} and their maxima, for both pHs.

Table 2 - Maximum and compressional modulus values at 30 mN m^{-1} of DPPE films on either PBS or acetate buffer pH 4.5 with different amounts of Ch35%

	C_S^{-1} at 30 mN m^{-1}		C_S^{-1}, max	
Concentration of Ch35%	**PBS**	**Acetate**	**PBS**	**Acetate**
0 mg mL^{-1}	203	240	354	367
10^{-5} mg mL^{-1}	175	213	337	369
10^{-3} mg mL^{-1}	165	244	286	404
10^{-1} mg mL^{-1}	70	126	192	235

Source: JOCHELAVICIUS (63)

In summary, we investigated the interaction between the two zwitterionic phospholipids (DPPC and DPPE) and Ch35% on Langmuir monolayers. Ch35% induced a shift in the pressure-area isotherms to higher molecular areas when its concentration was increased. At the highest Ch35% concentration, the compressional moduli decreased, indicating fluidization and penetration of the polymer into the monolayers. This decrease was kept even at 30 mn m^{-1}, which correlates with the pressure of a biomembrane. (3) Considering these isotherm measurements, the interaction with DPPE appears to be stronger, especially on acetate buffer. Even though the two lipids are structurally similar, the smaller headgroup enables DPPE molecules to pack tightly together, forming intermolecular H-bonds. When Ch35% is incorporated to the film, these bonds are hindered, and the change on the isotherm profile is highly evident. In general, the minimum concentration of Ch35% to produce visible changes on the isotherm curves is smaller on that buffer. This is related to the polycationic character of chitosans on acidic media, which contributes to interactions with the phosphate groups of the phospholipids headgroups. Once Ch35% can penetrate the monolayers, however, the disturbance caused on PBS subphases is greater, which is related to the larger volume occupied by Ch35% in this medium.

4.2 Anionic phospholipid and Ch35%

Similarly to what was observed for the zwitterionic lipids, the pressure-area isotherm of DPPG on both subphases, in the absence of Ch35%, starts as LE and achieves LC state in a

transition marked by a plateau. This plateau is larger on pH 7.4 than on pH 4.5, as shown in Figure 9. As discussed for DPPE in section 4.1, the headgroup of DPPG also forms intermolecular hydrogen bonds, but they are hindered by charge repulsion. (66) The compressional moduli in Figure 10 are higher for the acetate buffer. The higher values should be related to a reduction in charge repulsion on a more acidic media, as the monolayer molecules can stay closer to each other, forming a more rigid structure. In the presence of Ch35%, monolayer expansion is only significant for the highest concentration of Ch35% (10^{-1} mg mL^{-1}, on both pHs), as shown in Figure 9. This is somehow unexpected based on the literature and considering the polycationic character of Ch35% and the negatively charged headgroup of DPPG. Because of the opposite charges, a stronger interaction should be expected than with zwitterionic lipids, especially on acetate buffer. This expectation is not fulfilled because the number of charges in Ch35% is small to produce a stronger attraction, and other forces should be more significant. We infer from these results that the degree of acetylation (DA) is relevant for the interaction between chitosans and Langmuir monolayers. The expansion is larger on PBS, like in the previous cases, as the volume of Ch35% is larger on that buffer.

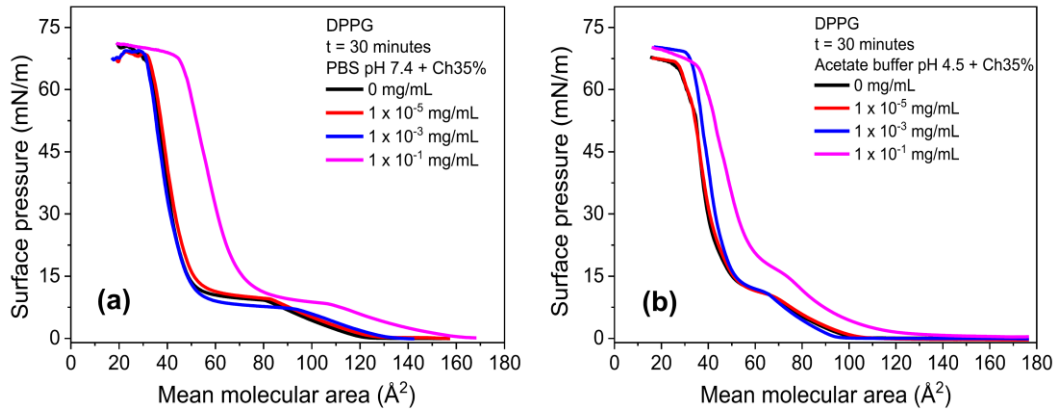

Figure 9 - Pressure-area isotherms of DPPG monolayers on PBS pH 7.4 (a) and acetate buffer (b) containing different concentrations of Ch35%

Source: JOCHELAVICIUS (63)

On acetate buffer, there is a slight increase in stabilization for the concentration of 10^{-3} mg mL^{-1}, verified by an increase in the collapse pressure (67), accompanied by an increase in the compressional modulus at high surface pressures (Figure 10b). For the highest concentration, the collapse pressure is similar to the curve without chitosan. The maximum value of the compressional modulus is smaller, however, despite the observed expansion. We believe that when a small quantity of Ch35% is present in the subphase, it may decrease charge

repulsion of DPPG headgroups at high surface pressures. On the other hand, when a higher quantity is present, it can penetrate the monolayer and interact with the lipid hydrocarbon chains, interfering in the monolayer organization. Also, at a high Ch35% concentration the phase transition occurs at smaller areas, which indicates that the monolayer stayed longer in the expanded state. On PBS, the compressional modulus was kept approximately the same for all concentrations of Ch35%, as seen in Figure 10a. Yet, the expansion in area was higher than on acetate. Table 3 shows the values for DPPG compressional moduli at 30 mN m^{-1} and their maximum values, taken from Figure 10.

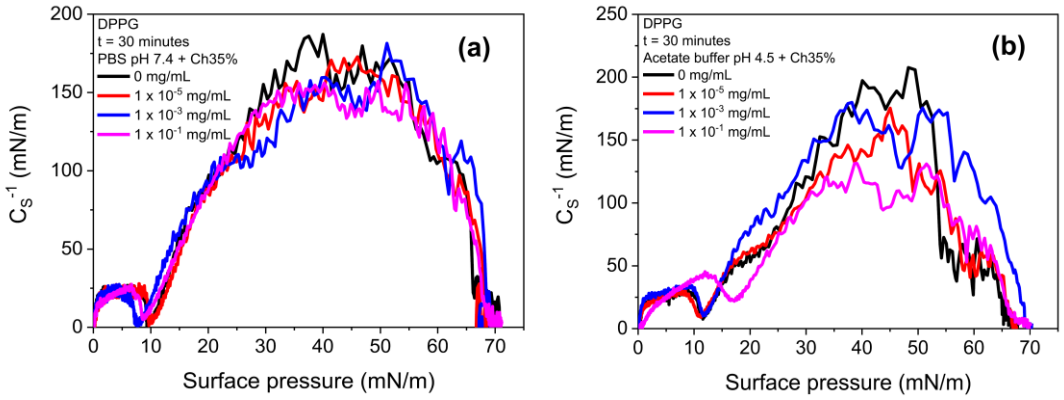

Figure 10 - Compressional moduli of DPPG π-A isotherms on PBS pH 7.4 (a) and acetate buffer (b) containing different concentrations of Ch35%
Source: JOCHELAVICIUS (63)

As briefly discussed in section 2, there is ample evidence in the literature that interaction of chitosan with lipid monolayers involves electrostatic and hydrophobic forces. In Pavinatto et al. study (46) in TS buffer pH 3.0, chitosans were found to penetrate the monolayer and interact with hydrocarbon tails and lipids headgroups. The two chitosans used in ref. (46) had a high MW with DA = 22% and a low MW, obtained by the depolymerization of the first one, with DA = 10%). Penetration into the monolayer was supported by PM-IRRAS spectra, and caused a decrease in both phospholipid ordering and density. The interaction was stronger with DPPG than with DPPC. They also verified by sum-frequency generation spectroscopy (SFG) that chitosan induced gauche defects on DPPG molecules (DPPC films were not investigated then), even though a high conformational order was still maintained. In a thermodynamics study, Krajewska *et al*. (52) also concluded that electrostatic and non-electrostatic interactions occur between chitosan (DA = 17%) and DPPG films, suggesting a predominance of non-electrostatic ones. They worked with subphases containing acetate buffers with pHs 3.5, 4.75 and 6.0, and a temperature range from 15 to 37°C. After a similar study with DPPC, at pHs 3.5

and 6.0, they concluded that the interactions are weaker than for DPPG and predominantly non-electrostatic. The change in behavior induced by interacting with chitosan was slightly increased at pH 6.0, contrary to DPPG monolayers, whose effects were more intense at pH 3.5. (51)

Table 3 - Maximum and compressional modulus values at 30 mN m^{-1} of DPPG films on either PBS or acetate buffer pH 4.5 with different amounts of Ch35%

	C_S^{-1} at 30 mN m^{-1}		**C_S^{-1}, max**	
Concentration of Ch35%	**PBS**	**Acetate**	**PBS**	**Acetate**
0 mg mL^{-1}	150	120	187	207
10^{-5} mg mL^{-1}	130	105	173	175
10^{-3} mg mL^{-1}	115	133	181	180
10^{-1} mg mL^{-1}	142	102	157	131

Source: JOCHELAVICIUS (63)

The isotherms presented here for the anionic phospholipid DPPG indicate that Ch35% can only produce significant changes at the highest concentration used (10^{-1} mg mL^{-1}). The intermediary concentration of 10^{-3} mg mL^{-1} on acetate buffer increased the collapse pressure and the rigidity near it, differently from what was observed with the highest chitosan concentration. Therefore, Ch35% at a small concentration should stabilize headgroups charge repulsion, but at high concentrations it can penetrate the film through the hydrocarbon chains, and interfere in their packing. On PBS, no changes in compressibility is identified, even though there is an area expansion. This indicates that chitosan molecules intercalate with DPPG molecules in the film without interfering in their intermolecular interactions. Since Ch35% exhibits a weak polycationic character and non-electrostatic interactions may play a more important role than electrostatic ones, according to the literature, we believe that this explains why there was no evidence for a stronger interaction between Ch35% and DPPG, compared to DPPC and DPPE, not even on an acidic pH.

4.3 *Escherichia coli* total lipid extract and Ch35%

The *E. coli* total lipid extract (identified by *E. coli*) is a natural and heterogeneous extract, containing lipids of varied types, sizes and saturation degrees. The main lipid classes encountered in the extract are PE, PG and CL (see section 3.2). PE is zwitterionic and PG and CL are anionic lipids. Structurally, CL is very distinguishable for having four hydrocarbon

chains (68) instead of two in DPPE and DPPG. This structure makes it bulky and hinders lipid packing. (69) Heterogeneity and the presence of CL – even in a relatively low quantity (~10% in mass) – combined, reflect in a very fluid monolayer. Figure 11 and Figure 12 show surface pressure-area isotherms and compressional moduli, typical of expanded monolayers, with no transition to the condensed phase. Similarly to eukaryote membrane models, monolayers formed by *E. coli* lipids present domain formation (70), but they are much more fluid. (71) In eukaryote models, cholesterol is present, which has a high packing capacity and confers condensation and ordering to monolayers containing phospholipids and/or sphingolipids. (72) The domains formed are called lipid rafts. (72-73)

Even though domains are reported in pure water, we found evidence in the literature that with NaCl in the aqueous subphase, Na^+ ions hamper the interaction between the molecules in monolayers containing PE, PG and CL. (68) This effect is a consequence of an increased electrostatic repulsion due to the release of counterions that were bound to the phospholipids, making them more anionic. The presence of other cations in the subphase (as the H^+ in acidic media) are supposed to produce a similar effect. What is observed is a higher excess area relatively to the ideal mixture and a positive Gibbs free energy. (68,74) A characteristic of films composed by POPE/POPG and POPE/DPPG is that the number of domains visualized by Brewster angle microscopy is smaller when there is CL in the mixtures. On subphases containing NaCl solution, this is intensified, and it is seen a homogenous phase during almost the whole course of the isotherm, except for small domains at a surface pressure near 30 mN m^{-1}. (68) Since we used subphases that contain Na^+ or H^+ ions, we believe that in our experiments the monolayers should be approximately homogeneous, with molecules away from each other due to a strong charge repulsion, hampering domain formation.

We could expect a strong interaction between Ch35% with the *E. coli* extract because of the anionic phospholipids PG and CL (about 25% in mass), especially in an acidic pH. However, as observed for DPPG monolayers, the expansion caused by Ch35% was more evident on PBS, as seen in Figure 11. The compressional moduli profile in Figure 12, nonetheless, suffered a more evident change in acetate buffer at surface pressures above 15 mN m^{-1}. The expanded phase is maintained with an increase in collapse pressure, also comparable with DPPG. From that condensing effect, one may infer that Ch35% in the acetate buffer made more attractive the interactions between the molecules of *E. coli* lipids. The exception is for the lowest Ch35% concentration (10^{-5} mg mL^{-1}), in which the collapse pressure decreased on both subphases. This indicates a small destabilization in the monolayers, which is a little surprising, considering the positive charges of Ch35% and the opposite effect verified for DPPG, when

there was a small concentration of chitosan. On PBS, a similar effect happens, with a decrease in collapse pressure for the lowest Ch35% concentration; for higher concentrations, the collapse appears close to the curve with no chitosan. The compressional moduli for the intermediary and the highest Ch35% concentrations exhibit a small increase at pressures above 25 mN m^{-1}, but it is only relevant close to 30 mN m^{-1} for 10^{-3} mg mL^{-1}. The values for the compressional moduli are given in Table 4. It seems from the isotherms and compressibility changes that Ch35% does not penetrate the *E. coli* monolayer on acetate buffer, interacting preferentially with the headgroups, and reducing charge repulsion. Except for the highest concentration (10^{-1} mg mL^{-1}), in which there is area expansion. On PBS, on the other hand, Ch35% can penetrate and interact with the hydrocarbon tails, since there is a considerable area expansion for 10^{-3} mg mL^{-1} and, an even higher, for 10^{-1} mg mL^{-1}. However, it does not change monolayer elasticity, not interfering in the intermolecular interactions but intercalating with the lipid molecules. This can be confirmed with PM-IRRAS (75-76) or SFG analysis (77), for example. As in the previous cases, the larger volume occupied by Ch35% in PBS when compared to acetate buffer contributes to the larger area expansion.

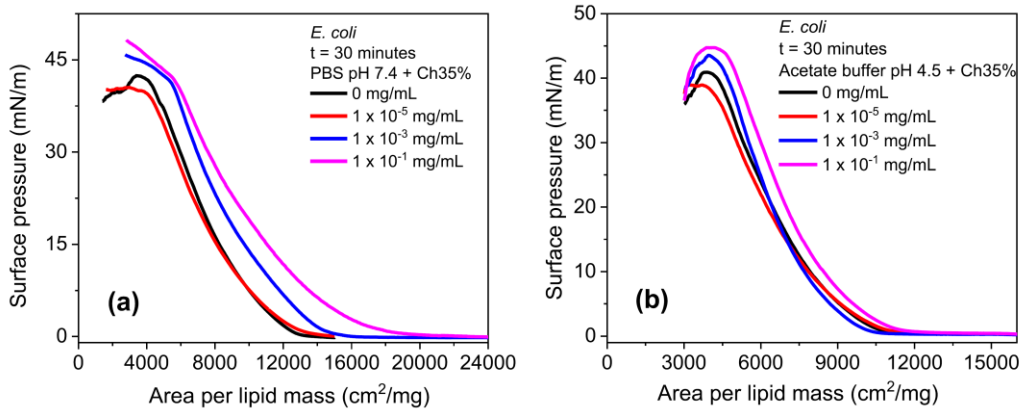

Figure 11 - Pressure-area isotherms of *E. coli* total lipid extract monolayers on PBS pH 7.4 (a) and acetate buffer (b) containing different concentrations of Ch35%
Source: JOCHELAVICIUS (63)

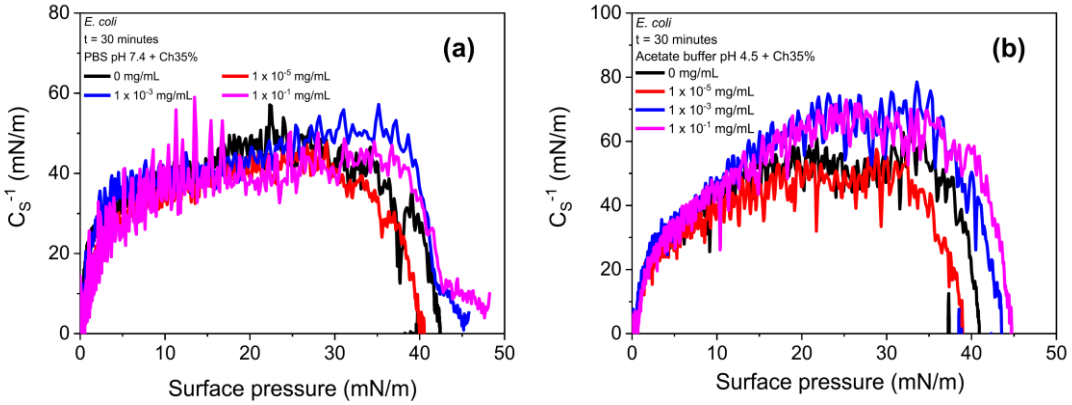

Figure 12 - Compressional moduli of *E. coli* total lipid extract on PBS pH 7.4 (a) and acetate buffer (b) containing different concentrations of Ch35%
Source: JOCHELAVICIUS (63)

The major difference in behavior for *E. coli* lipids compared to the previous monolayers studied here is that their highly fluid monolayers become less fluid in the presence of Ch35%. On acetate buffer, the *E. coli* monolayers are more stable for high concentrations of Ch35%, in contrast to the results for DPPG. This indicates that Ch35% reduces charge repulsion and facilitates lipid packing. From our previous results and from the literature, one notes that only unsaturated fatty acids monolayers (40) and the mixture containing SM-DPPC-Chol (1:1:1) (11) behave similarly, i.e. have their compressional moduli increased. The study with SM-DPPC-Chol (1:1:1) involved Ch35% and the one with fatty acids a chitosan with DA of 30% (see section 2). These DAs are higher than for most chitosans studied in the literature and discussed in Section 2. Also, for unsaturated DOPC monolayers (54), there is no increase (or a reduction) in the compressional modulus, and the authors used a chitosan with a lower DA (18%). However, the monolayer expansion was also small, so maybe a higher amount of this chitosan or a higher waiting time before compression (they allowed only 10 min) could produce the same fluidization effect. Another characteristic that is common to *E. coli*, SM-DPPC-Chol (1:1:1) and unsaturated fatty acids monolayers is the considerably high fluidity. In fluid monolayers, the lipids probably do not pack easily, leaving spaces between the molecules even at high surface pressures. Hence, intermolecular interactions should be weaker than in condensed monolayers. Therefore, chitosan molecules have more freedom to allocate between the molecules in the film, and this may induce a higher ordering, producing higher rigidity.

Table 4 - Maximum and compressional modulus values at 30 $mN\ m^{-1}$ of *E. coli* total lipid extract films on either PBS or acetate buffer pH 4.5 with different amounts of Ch35%.

	Cs^{-1} at 30 mN m^{-1}		$Cs^{-1}_{, max}$	
Concentration of Ch35%	**PBS**	**Acetate**	**PBS**	**Acetate**
0 mg mL^{-1}	42	50	49	58
10^{-5} mg mL^{-1}	40	51	45	52
10^{-3} mg mL^{-1}	50	66	51	73
10^{-1} mg mL^{-1}	40	63	45	70

Source: JOCHELAVICIUS. (63)

Even though fluidity is a common aspect for the monolayers mentioned in the last paragraph, the mixture SM-DPPC-Chol (1:1:1) is known to form lipid rafts, so we can find isles of lipids that are close to each other, interacting strongly, and regions less condensed between them. Therefore, as for the DPPE monolayers reported in section 4.1, the incorporation Ch35% could disrupt these interactions, and cause the molecules in the domain regions to move further apart, expanding the area occupied by them. However, instead of decreasing, this increases the compressional modulus, probably by making the regions between domains smaller. In contrast, the molecules in the approximately homogenous *E. coli* film interact loosely, and Ch35% molecules do not interfere much in their organization. The compressional modulus is higher for SM-DPPC-Chol (1:1:1) than on *E. coli* monolayers, mainly on PBS. In addition, Ch35% induces phase transition, and, unlike for *E. coli* lipids, the changes in elasticity are higher on PBS. In fact, Ch35% induced measurable expansion on SM-DPPC-Chol (1:1:1) monolayers starting at 10^{-4} mg mL^{-1} for PBS and 10^{-6} mg mL^{-1} for acetate buffer. (11) The strong effect on SM-DPPC-Chol (1:1:1) monolayers, mammal membrane mimetic, suggests that careful studies have to be performed to apply chitosan as an antimicrobial agent for its use in medicine, for example, avoiding side effects.

In summary, the highly fluid monolayer of *E. coli* lipids was only slightly influenced by Ch35%. On PBS, there was a significant expansion for the highest concentrations of Ch35% (10^{-3} and 10^{-1} mg mL^{-1}), but no considerable change on the compressibility profile. In contrast, on acetate buffer only a small expansion is observed, with the more evident effects being the increase in collapse pressure and in the slope of the curves. This suggests an increased stability and condensation, even though the liquid expanded state was maintained. Table 5 lists the films studied here and in ref. (11), with the minimum concentration of Ch35% necessary to produce visible effects on each pH.

Table 5- Minimum concentration of Ch35% in the subphase to have measurable effect on lipid monolayers.

Lipid	pH	Minimum concentration for interaction
DPPC	7.4	10^{-1} mg mL^{-1}
DPPE	7.4	10^{-3} mg mL^{-1}
DPPG	7.4	10^{-1} mg mL^{-1}
E. coli	7.4	10^{-3} mg mL^{-1}
SM-DPPC-chol(1:1:1)	7.4	10^{-4} mg mL^{-1}
DPPC	4.5	5×10^{-3} mg mL^{-1}
DPPE	4.5	10^{-5} mg mL^{-1}
DPPG	4.5	10^{-3} * mg mL^{-1}
E. coli	4.5	10^{-3} * mg mL^{-1}
SM-DPPC-chol(1:1:1)	4.5	10^{-6} mg mL^{-1}

*There are measurable modifications in compressibility and collapse pressure, but they are small compared to other lipids. For DPPG, the highest concentration of Ch35% (10^{-1} mg mL^{-1}) expresses a more visible modification.
Source: JOCHELAVICIUS (63)

Since there are questions about the impact of the DA of Ch35% on its stronger effect on neutral membrane models, we decided to study a chitosan with 15% of acetylation (Ch15%), using the more realistic models (*E. coli* lipid extract and the mixture that forms rafts) and the LPS from the outer membrane of *E. coli*. The latter was investigated because we wanted to test the hypothesis that chitosan can interact more strongly with the outer membrane, instead of the inner membrane. We, therefore, started with the Ch35% in LPS monolayers.

4.4 Lipopolysaccharide and Ch35%

LPS is a component of the outer membrane of Gram-negative bacteria, having a net-negative charge. It is the most external component of a bacterium, and interacting with it is important for a molecule to act as an antimicrobial agent, without using a porin channel. For a large molecule such as a polysaccharide, this interaction is key for its application. We first discuss the isotherms of LPS without Ch35%. LPS is soluble in water, therefore, on a subphase of pure water, it does not form a monolayer, but rather migrates to the subphase. However, on PBS or acetate buffer, there is monolayer formation. The surface pressure-area isotherms are shown in Figure 13, featuring smooth curves with no phase transition plateaus on both pHs. The compressional modulus curves in Figure 14 indicate the expanded nature of the isotherms, with maxima a little higher than *E. coli* lipids monolayers. Comparing between the two subphases, the maximum value is higher on PBS, while for *E. coli* it is lower (see Figure 12).

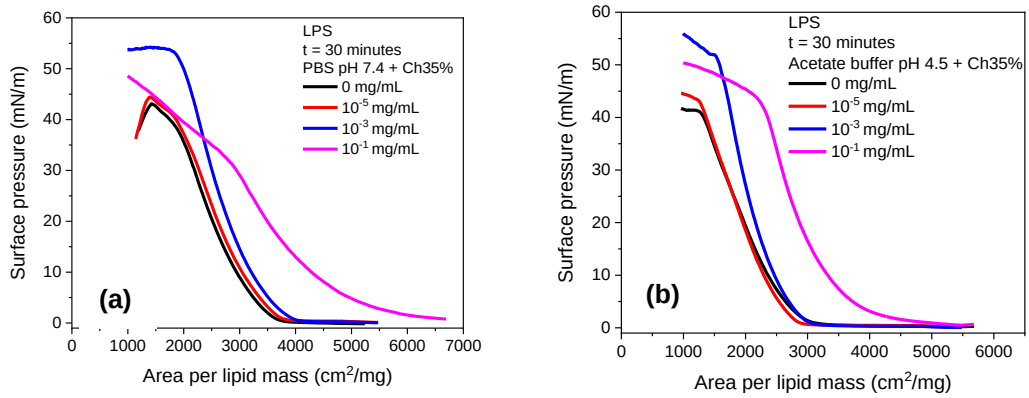

Figure 13 - Pressure-area isotherms of LPS monolayers on PBS pH 7.4 (a) and acetate buffer (b) containing different concentrations of Ch35%

Source: By the author

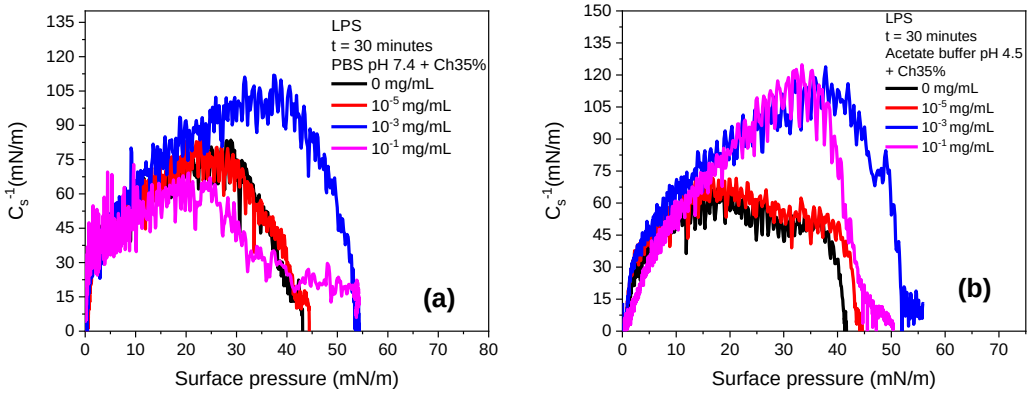

Figure 14 - Compressional moduli of LPS on PBS pH 7.4 (a) and acetate buffer (b) containing different concentrations of Ch35%

Source: By the author

In the presence of Ch35% in the subphases, there is an area expansion shown in Figure 13 for the intermediary and highest Ch35% concentrations (10^{-3} and 10^{-1} mg mL^{-1}), confirming Ch35% penetration. For 10^{-3} mg mL^{-1}, there is an increase in the slope, which is verified as an increase in the compressional modulus in Figure 14. The collapse pressure also increases for both pHs. The lift-off area, however, is only slightly increased on PBS. Therefore, with Ch35% incorporation the molecules in the film still occupy the same area as without it, at low surface pressures. As the monolayer is compressed, the area increases with Ch35% incorporation, but the monolayer is more rigid than without Ch35%. Figure 14 shows a transition to the LC phase for both pHs, with monolayer condensation and a higher stability upon incorporating Ch35%. On acetate, the increase in compressional modulus was much higher than on PBS. In the beginning of the compression, the monolayer is fluid, then becoming condensed at high pressures. For 10^{-1} mg mL^{-1}, however, the results are somewhat different. Both isotherms were

shifted to higher molecular areas, with a larger increase of the lift-off area on PBS (Figure 13). On this subphase, fluidization occurs for the monolayer. There is a change in the slope around 30 mN m^{-1}, which does not seem like a collapse but rather a change in molecular orientation. Figure 14 shows a decrease in the modulus but it does not achieve zero, as it happens in the collapse (the derivative becomes positive, so the compressional modulus becomes negative, crossing the x-axis). Ch35% must have induced a tilt in the film molecules to produce this change in slope. Further analysis with PM-IRRAS and SFG could give us a better idea of what is happening in this region of the isotherm. On acetate, compressibility is similar to that of the intermediary concentration but the collapse is achieved earlier, indicating a decrease in stabilization (still higher than without Ch35%).

The data on compressional moduli at 30 mN m^{-1} are summarized in Table 6. Overall, we can conclude that Ch35% is incorporated to the LPS monolayers. At a small quantity, it is capable of increasing stability and decreasing repulsion between the molecules. This trend is sustained for higher amounts of chitosan on acetate, but the stability is partially decreased. On PBS, higher amounts of Ch35% change the interactions between the molecules in the film, increasing even more the monolayer fluidity and promoting a change in their orientation. The affinity for chitosan to LPS monolayers does not seem to be stronger at a specific pH.

Table 6 - Maximum and compressional modulus values at 30 mN m^{-1} of LPS films on either PBS or acetate buffer pH 4.5 with different amounts of Ch35%.

	C_S^{-1} at 30 mN m^{-1}		**C_S^{-1}, max**	
Concentration of Ch35%	**PBS**	**Acetate**	**PBS**	**Acetate**
0 mg mL^{-1}	73	42	80	63
10^{-5} mg mL^{-1}	69	57	79	67
10^{-3} mg mL^{-1}	97	110	104	113
10^{-1} mg mL^{-1}	44	105	64	111

Source: By the author

In a comparison between the results for LPS and those in the previous sections, we may conclude that the affinity of Ch35% on LPS monolayers is stronger, since a lower concentration of this chitosan generates more visible changes in the isotherms. However, when compared with SM-DPPC-Chol (1:1:1), studied in (11), the affinity is considerably weaker. The combination of these factors corroborates the hypothesis that the DA of this chitosan is too high for electrostatic interactions to have a significant impact on its action.

4.5 *Escherichia coli* total lipid extract and Ch15%

The isotherms for *E. coli* lipids reveal a fluid profile of the monolayers, as can be seen in Figure 15 and Figure 16. Similarly to Ch35%, the incorporation of Ch15% causes area expansion, but the effect on *E. coli* lipids is more visible for Ch15%. On PBS, with 10^{-5} mg mL^{-1} of Ch15% there is a slight expansion in molecular area, not very significant. For 10^{-3} mg mL^{-1}, there is a very significant expansion, accompanied of a significant increase in collapse pressure (Figure 15a), higher than for Ch35% in Figure 11a. The compressional modulus in Figure 16a increases with incorporation of Ch15%, mainly for pressures above 15 mN m^{-1}, even though the expanded state is kept. The increased stability should be related to two factors: a reduction in charge repulsion in the headgroups region, and the interaction with the hydrophobic tails, facilitating their packing. The data for the compressional modulus are given Table 7. For the highest concentration (10^{-1} mg mL^{-1}), the compressional modulus decreases, becoming similar to the curve without Ch15%. The collapse, nonetheless, occurs in a higher surface pressure (similar to the intermediary concentration). The lift-off area is larger, but the molecular area in which the collapse occurs is closer to the intermediary Ch15% concentration, indicating that part of the chitosan molecules are expelled back to the subphase at high surface pressures. On acetate buffer in Figure 15a, for 10^{-5} mg mL^{-1} of Ch15%, there is a slight expansion on the lift-off area, and a slight decrease in the slope, verified by a decrease in the compressional modulus in Figure 16b. At 30 mN m^{-1}, this is not significant. When 10^{-3} mg mL^{-1} of Ch15% is present in the subphase, the lift-off area is close to that of 10^{-5} mg mL^{-1} isotherm. There is, however, an increase in the slope that generates an increase in the compressional modulus. As on PBS, there is no phase transition and the collapse pressure is higher than without Ch15%, but the changes in compressibility, collapse pressure and molecular area are much more evident on PBS. This indicates that for *E. coli* lipids non-electrostatic forces must play a more important role when it comes to interaction with Ch15%. For 10^{-1} mg mL^{-1}, the lift-off area is considerably larger (the expansion is still smaller than on PBS) and the compressional modulus decreases slightly, until a pressure of about 22.5 mN m^{-1}. At higher pressures, the modulus is higher than without chitosan because the collapse is achieved later, and the collapse pressure is slightly higher than for 10^{-3} mg mL^{-1}. The effect on acetate is also more expressive for Ch15% than for Ch35%. The diameter of the Ch15% in PBS is 23.7 ± 1.2 nm, and, on acetate buffer, 16.8 ± 0.7 nm. (10)

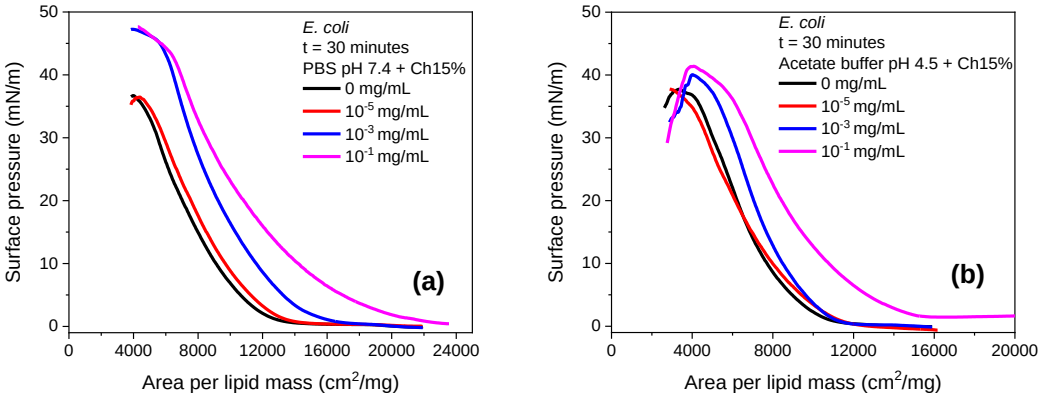

Figure 15 - Pressure-area isotherms of *E. coli* total lipid extract monolayers on PBS pH 7.4 (a) and acetate buffer (b) containing different concentrations of Ch15%

Source: By the author

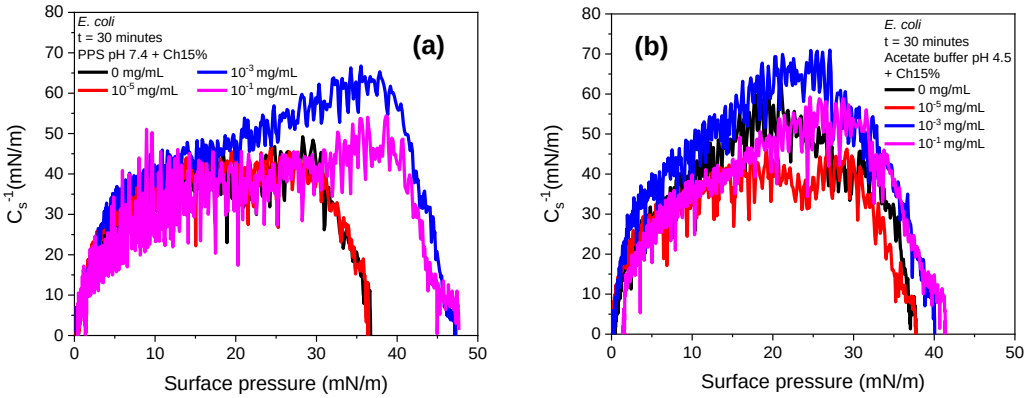

Figure 16 - Compressional moduli of *E. coli* total lipid extract on PBS pH 7.4 (a) and acetate buffer (b) containing different concentrations of Ch15%

Source: By the author

Table 7 - Maximum and compressional modulus values at 30 mN m^{-1} of *E. coli* total lipid extract films on either PBS or acetate buffer pH 4.5 with different amounts of Ch35%.

	C_S^{-1} at 30 mN m^{-1}		**C_S^{-1}, max**	
Concentration of Ch35%	**PBS**	**Acetate**	**PBS**	**Acetate**
0 mg mL^{-1}	42	42	46	57
10^{-5} mg mL^{-1}	38	43	45	45
10^{-3} mg mL^{-1}	58	47	64	67
10^{-1} mg mL^{-1}	39	53	51	56

Source: By the author

4.6 Lipopolysaccharide and Ch15%

Herein, we only have results on subphases containing acetate buffer, as mentioned in section 3.2. For Ch15% in the subphase, Figure 17 shows a shift to higher molecular areas even at the smallest concentration used (10^{-5} mg mL^{-1}). These are the most evident shifts until now, comparing to the previous results presented. Initially, at the lowest concentration, there is a small destabilization of the LPS monolayer, having its collapse pressure reduced. With 10^{-3} mg mL^{-1} of Ch15%, the lift-off area is similar to the 10^{-5} mg mL^{-1} curve, but the collapse pressure increases and so does the compressional modulus, even though the condensed phase is still not achieved (see Figure 18). This indicates that, even though there is more chitosan, the area occupied by the films at zero pressure are equivalent. However, as the pressure increases, the area occupied also increases, and there are condensation and stabilization effects. With 10^{-1} mg mL^{-1} in the subphase, the lift-off area increases considerably. This area increase is maintained through the course of the isotherm, which means that more Ch15% molecules could penetrate the monolayer and they were not expelled. The data on the compressibility modulus are shown in Table 8. The compressibility and the collapse pressure were similar to the intermediary Ch15% concentration curve, indicating that there were no significant changes in intermolecular interactions for the two concentrations. Therefore, Ch15% causes expansion and makes the LPS monolayer in acetate buffer more rigid and stable until a certain amount (between 10^{-5} mg mL^{-1} and 10^{-3} mg mL^{-1} in the subphase). A higher amount is capable of penetrating and intercalating with the film molecules, without changing their structure.

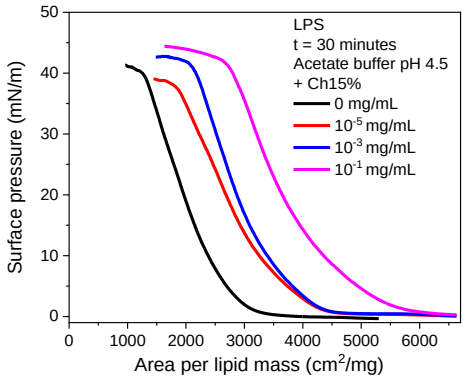

Figure 17 - Pressure-area isotherms of LPS monolayers on acetate buffer containing different concentrations of Ch15%

Source: By the author

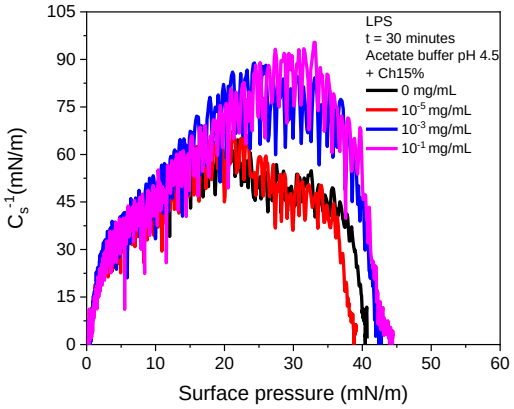

Figure 18 - Compressional moduli of LPS on PBS and acetate buffer containing different concentrations of Ch15%
Source: By the author

As we expected, the effect of Ch15% is also higher on LPS monolayers than with Ch35% (at least on acetate buffer). The difference here is much more evident than for *E. coli* lipids monolayers. Even though we do not have data on PBS, it is indicative that electrostatic interactions between LPS and Ch15% play an important role, contrasting to *E. coli* lipids. The higher protonation of Ch15%, in comparison with Ch35%, determines a considerably higher affinity for LPS molecules. This suggests that the interaction with the LPS from the outer membrane of Gram-negative bacteria should be relevant to the action of chitosan as an antimicrobial agent. Another type of molecule that could be relevant for chitosan action is the peptidoglycan from the cell wall, mainly for Gram-positive bacteria.

Table 8 - Maximum and compressional modulus values at 30 $mN\ m^{-1}$ of LPS films on acetate buffer pH 4.5 with different amounts of Ch35% (values on PBS are not available).

	Cs^{-1} at 30 mN m^{-1}	**Cs^{-1}, max**
Concentration of Ch35%	**Acetate**	**Acetate**
0 mg mL^{-1}	47	61
10^{-5} mg mL^{-1}	39	64
10^{-3} mg mL^{-1}	75	86
10^{-1} mg mL^{-1}	83	92

Source: By the author

4.7 Extra data on lipid rafts

The results for Ch15% obtained in the previous sections can be compared to unpublished data kindly provided to us by Dr. Andressa Pereira on lipid rafts (SM-DPPC-Chol (1:1:1)) Langmuir monolayers on PBS. The isotherms she obtained are plotted in Figure 19. The effects from Ch15% are concentration dependent. For 10^{-5} mg mL^{-1} Ch15%, there is a significant expansion of the isotherm lift-off area, but the isotherm coincides with the one taken with the SM-DPPC-Chol (1:1:1) mixture at high pressures. Hence, Ch15% seems to be expelled from the monolayer at about 35 mN m^{-1}, and cause destabilization because the collapse pressure is slightly lower than for monolayer without Ch15%. At the intermediary concentrations, there is expansion, but the lift-off areas and the fluidization effect are smaller than with 10^{-5} mg mL^{-1} of Ch15%. At 10^{-4} mg mL^{-1} Ch15% also seems to be expelled from the monolayer at high pressures. For the highest concentration (10^{-1} mg mL^{-1}), the lift-off area is the biggest, and the area increase persists until the end of the isotherm. There is a fluidization effect as well, smaller than for the lowest concentration, but these two isotherms do not achieve the condensed state, as the others.

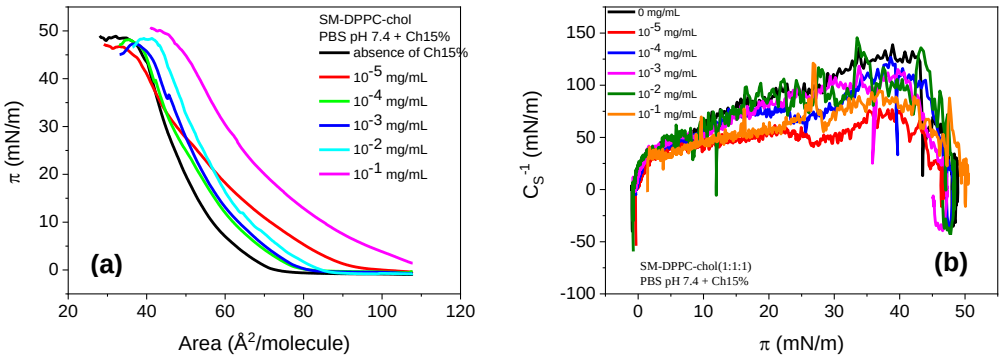

Figure 19 - Pressure-area isotherms (a) and compressional moduli as a function of the surface pressure (b) of SM-DPPC-Chol (1:1:1) monolayers on PBS pH 7.4 containing different concentrations of Ch15%
Source: PEREIRA (data not published)

Considering all the data presented here, from references (11,63) and the unpublished material, we organized the isotherms as in Figure 20. The pressure-area isotherms are ordered according to the ones that required the smallest concentrations of either chitosan to produce visible effects. Only part of the monolayers are shown, and the ones that are not in the figure required higher concentrations. LPS on acetate buffer with Ch15% is the first, followed by SM-DPPC-Chol (1:1:1) on PBS with Ch15%. It is worth reminding that we do not have results on acetate for the latter and on PBS for the former. Also, neat phospholipids were only used in subphases with Ch35%. Overall, we note that Ch15% induces stronger effects than Ch35%, but

surprisingly for *E. coli* lipid extract monolayers the effect of Ch15% is stronger at a physiological pH. The smallest concentration necessary to produce effects is similar on both pHs. The charged LPS monolayer on acetate buffer was mostly affected, but the mixture that forms rafts on PBS was not far behind; unfortunately, we do not have data for them on the same subphase. However, at 30 mN m^{-1}, the expansion caused by this mixture is not as significant as for LPS. Since LPS is charged and for Ch35% the effect on acetate buffer was considerably stronger, we expect it to have higher affinity for Ch15% on acetate. SM-DPPC-Chol (1:1:1) is neutral, therefore the difference between the two media might not be that relevant. Even so, as the affinity is close for these two kinds of membrane models we suggest that the action of chitosan as antibacterial agent could also be related to other factors, besides the interaction with the membrane. In other words, the selectivity of chitosans over bacterial cells relative to mammal cells could have other contributions in addition to electrostatic interactions between opposite charges in chitosan and in the membrane. Furthermore, charge distribution in the chitosan surface could be relevant to explain peculiar effects discussed here. Of course, as emphasized, there are also peptidoglycans in bacteria cell walls, which can interact with chitosans, and their affinity can be tested in Langmuir monolayers.

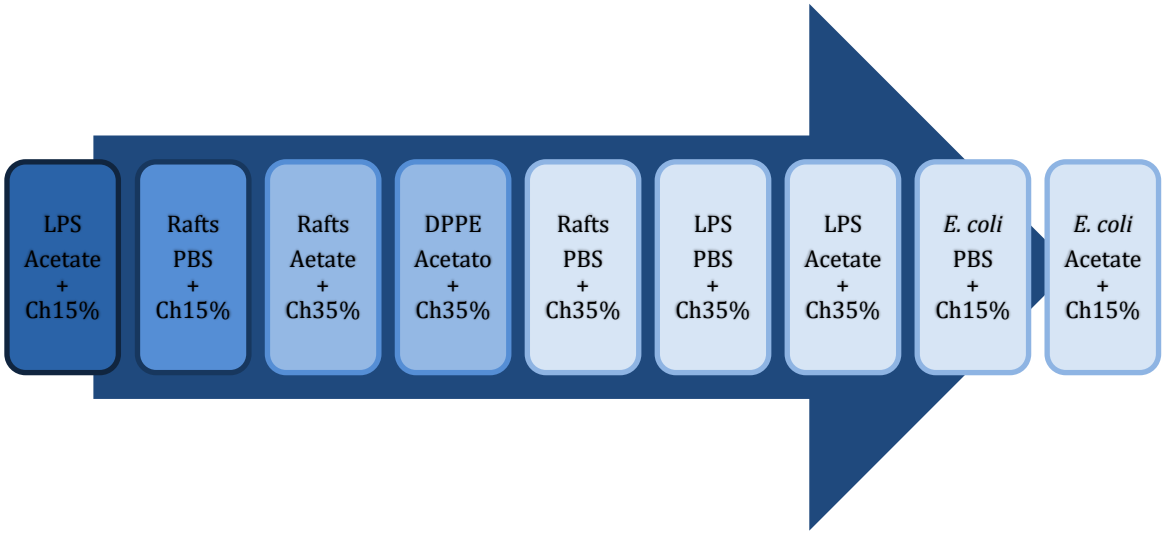

Figure 20 - Monolayers studied here, on different subphases, ordered according to their affinity for Ch15% or Ch35%. Blocks are colored in a gradient of blue, from higher to lower affinity. Same color blocks represent monolayers equivalent in affinity.
Source: By the author

5 CONCLUSIONS

In this thesis, we discussed the interaction of two chitosans with different degrees of acetylation with lipid monolayers. We chose monolayers that represent more realistic models, in comparison to neat phospholipids. The models used prior to our studies were shown to be limited, and do not satisfactorily explain the higher affinity of some chitosans to bacterial cells, relative to mammal cells. Also, with fully water-soluble chitosans it was possible to work at a physiological pH. This is relevant while dealing with living organisms, as necessary for many chitosan applications. The charge distribution in those chitosans is different from the others because of a quasi-random pattern of acetylation. The pattern of acetylation, combined with the DA, the molecular weight and the dispersity, drives the use of each chitosan.

The results provided here represent an advance in our understanding on why some chitosans are selective over bacterial cells, in comparison to mammal cells. Even though our work created more questions and did not completely solve them, we showed that the explanations found previously in the literature are not satisfactory. They indeed can explain the results observed for those monolayers and chitosans, in particular. However, they cannot offer a global explanation of the factors that will determine higher selectivity over bacteria *in vivo*. The interaction of chitosans with inner membrane lipids is not an adequate system to investigate the action of these polysaccharides in bacteria. The use of LPS and, possibly, peptidoglycan has to be considered. In our work, we could confirm that the number of charges influences the effect produced by chitosan in lipid monolayers. This correlates with the higher bactericidal activity verified for chitosans with higher availability of charged groups. (78) To complement our studies, besides obtaining results for LPS on PBS, we can combine with the Langmuir studies techniques that allow us to obtain molecular-level information, such as PM-IRRAS and SFG. This could clarify the contribution of electrostatic and non-electrostatic interactions for the chitosans incorporation. In addition, combining *in vivo* evidence, an appropriate mode of action could be proposed.

After this work has been completed, questions were raised about whether we can affirm that the results obtained diverge from the prior scientific literature or not. Are not them a mere consequence of how we outlined our experiments, elucidating that minor differences in experimental setups may change our way of seeing things? Do not they simply highlight multiple angles and peculiarities that describe complex biological events? In fact, the outcomes may not diverge, but complementary. We now have more tools to understand and investigate the action of chitosans in cellular membranes.

REFERENCES

1 ELDERDFI, M.; SIKORSKI, A. F. Langmuir-monolayer methodologies for characterizing protein-lipid interactions. **Chemistry and Physics of Lipids**, v. 212, p. 61–72, 2018. DOI: 10.1016/j.chemphyslip.2018.01.008.

2 MAGET-DANA, R. The monolayer technique: a potent tool for studying the interfacial properties of antimicrobial and membrane-lytic peptides and their interactions with lipid membranes. **Biochimica et Biophysica Acta (BBA) -** biomembranes, v. 1462, n. 1, p. 109–140, 1999.

3 PEETLA, C.; STINE, A.; LABHASETWAR, V. Biophysical interactions with model lipid membranes: applications in drug discovery and drug delivery. **Molecular Pharmaceutics**, v. 6, n. 5, p. 1264–1276, 2009.

4 FENDLER, J. H. Interactions and kinetics in membrane mimetic systems. **Annual Review of Physical Chemistry**, v. 35, n. 1, p. 137–157, 1984.

5 MARTINOTTI, C. *et al*. Molecular dynamics simulation of small molecules interacting with biological membranes. **ChemPhysChem**, v. 21, n. 14, p. 1486–1514, 2020.

6 VENABLE, R. M.; KRÄMER, A.; PASTOR, R. W. Molecular dynamics simulations of membrane permeability. **Chemical Reviews**, v. 119, n. 9, p. 5954–5997, 2019.

7 PASTOR, R. W. Molecular dynamics and Monte Carlo simulations of lipid bilayers. **Current Opinion in Structural Biology**, v. 4, n. 4, p. 486–492, 1994.

8 LI, D.; ZHOU, B.; LV, B. Antibacterial therapeutic agents composed of functional biological molecules. **Journal of Chemistry**, v. 2020, p. 6578579, 2020. DOI: 10.1155/2020/6578579.

9 BAKSHI, P. S. *et al*. Chitosan as an environment friendly biomaterial – a review on recent modifications and applications. **International Journal of Biological Macromolecules**, v. 150, p. 1072–1083, 2020. DOI: 10.1016/j.ijbiomac.2019.10.113.

10 FIAMINGO, A.; CAMPANA FILHO, S. P.; OLIVEIRA JUNIOR, O. N. Tuning the properties of high molecular weight chitosans to develop full water solubility within a wide pH range. **ChemRxiv,** 2020. Available from: https://chemrxiv.org/engage/api-gateway/chemrxiv/assets/orp/resource/item/60c7480f0f50db6b0d3966f9/original/tuning-the-properties-of-high-molecular-weight-chitosans-to-develop-full-water-solubility-within-a-wide-p-h-range.pdf. Accessible at: 23 Jan. 2021.

11 PEREIRA, A. R. *et al*. Enhanced chitosan effects on cell membrane models made with lipid raft monolayers. **Colloids and Surfaces B:** biointerfaces, v. 193, p. 1111017, 2020.

12 WYDRO, P.; FLASIŃSKI, M.; BRONIATOWSKI, M. Molecular organization of bacterial membrane lipids in mixed systems - a comprehensive monolayer study combined with Grazing incidence X-ray diffraction and Brewster Angle Microscopy experiments. **Biochimica et Biophysica Acta** - biomembranes, v. 1818, n. 7, p. 1745–1754, 2012.

13 ZACHOWSKI, A. Phospholipids in animal eukaryotic membranes: transverse asymmetry and movement. **Biochemical Journal**, v. 294, n. 1, p. 1–14, 1993.

14 SINGER, S. J.; NICOLSON, G. L. The fluid mosaic model of the structure of cell

membranes. **Science**, v. 175, n. 4023, p. 720–731, 1972.

15 NICOLSON, G. L. The fluid - mosaic model of membrane structure: still relevant to understanding the structure, function and dynamics of biological membranes after more than 40 years. **Biochimica et Biophysica Acta** - biomembranes, v. 1838, n. 6, p. 1451–1466, 2014.

16 ALVES, A. C. *et al*. Biophysics in cancer: the relevance of drug-membrane interaction studies. **Biochimica et Biophysica Acta** - biomembranes, v. 1858, n. 9, p. 2231–2244, 2016.

17 BREZESINSKI, G.; MÖHWALD, H. Langmuir monolayers to study interactions at model membrane surfaces. **Advances in Colloid and Interface Science**, v. 100–102, p. 563–584, 2003. DOI: 10.1016/s0001-8686(02)00071-4.

18 STEFANIU, C.; BREZESINSKI, G.; MÖHWALD, H. Langmuir monolayers as models to study processes at membrane surfaces. **Advances in Colloid and Interface Science**, v. 208, p. 197–213, 2014. DOI: 10.1016/j.cis.2014.02.013.

19 MENDELSOHN, R.; MAO, G.; FLACH, C. R. Infrared reflection-absorption spectroscopy: principles and applications to lipid-protein interaction in Langmuir films. **Biochimica et Biophysica Acta -** biomembranes, v. 1798, n. 4, p. 788–800, 2010.

20 NOBRE, T. M. *et al*. Interactions of bioactive molecules & nanomaterials with Langmuir monolayers as cell membrane models. **Thin Solid Films**, v. 593, p. 158–188, 2015. DOI: 10.1016/j.tsf.2015.09.047.

21 PEDROSA, M.; MALDONADO-VALDERRAMA, J.; GÁLVEZ-RUIZ, M. J. Interactions between curcumin and cell membrane models by Langmuir monolayers. **Colloids and Surfaces B:** biointerfaces, v. 217, p. 112636, 2022. DOI: 10.1016/j.colsurfb.2022.112636.

22 PEREIRA, A. R.; SHIMIZU, F. M.; OLIVEIRA, O. N. Cholesterol modulates the interaction between paclitaxel and Langmuir monolayers simulating cell membranes. **Colloids and Surfaces B**: biointerfaces, v. 205, p. 111889, 2021. DOI: 10.1016/j.colsurfb.2021.111889

23 MILDNER, J.; WNĘTRZAK, A.; DYNAROWICZ-LATKA, P. Cholesterol and cardiolipin importance in local anesthetics–membrane interactions: the Langmuir monolayer study. **Journal of Membrane Biology**, v. 252, n. 1, p. 31–39, 2019.

24 MACHADO, A. C.; CASELI, L. Interaction of nitrofurantoin with lipid langmuir monolayers as cellular membrane models distinguished with tensiometry and infrared spectroscopy. **Colloids and Surfaces B-**biointerfaces, v. 188, p. 110794, 2020. DOI: 10.1016/j.colsurfb.2020.110794.

25 GRAVEL-TATTA, L.; DEWOLF, C.; BADIA, A. Are plant-based carbohydrate nanoparticles safe for inhalation? investigating their interactions with the pulmonary surfactant using Langmuir monolayers. **Langmuir**, v. 37, n. 42, p. 12365–12376, 2021.

26 PERCZYK, P.; GAWLAK, R.; BRONIATOWSKI, M. Interactions of fungal phospholipase Lecitase ultra with phospholipid Langmuir monolayers – search for substrate specificity and structural factors affecting the activity of the enzyme. **Biochimica et Biophysica Acta -** biomembranes, v. 1863, n. 10, p. 183687, 2021.

27 SCHMIDT, T. F. *et al*. Dengue fusion peptide in Langmuir monolayers: a binding

parameter study. **Biophysical Chemistry**, v. 271, p. 106553, 2021. DOI: 10.1016/j.bpc.2021.106553.

28 KRAJEWSKA, M.; DOPIERAŁA, K.; PROCHASKA, K. Lipid-protein interactions in Langmuir monolayers under dynamically varied conditions. **Journal of Physical Chemistry B**, v. 124, n. 1, p. 302–311, 2020.

29 MARTINS, B. A. *et al*. Penicillin-binding proteins (PBPs) determine antibiotic action in Langmuir monolayers as nanoarchitectonics mimetic membranes of methicillin-resistant Staphylococcus aureus. **Colloids and Surfaces B**: biointerfaces, v. 214, p. 112447, 2022. DOI: 10.1016/j.colsurfb.2022.112447.

30 SHRIVASTAVA, A. Polymerization. *In*: SHRIVASTAVA, A. (ed.). **Plastics design library**. New York: Elsevier, 2018. p. 17–48.

31 SORLIER, P. *et al*. Relation between the degree of acetylation and the electrostatic properties of chitin and chitosan. **Biomacromolecules**, v. 2, n. 3, p. 765–772, 2001.

32 KUMAR, A.; VIMAL, A.; KUMAR, A. Why chitosan? from properties to perspective of mucosal drug delivery. **International Journal of Biological Macromolecules**, v. 91, p. 615–622, 2016. DOI: 10.1016/j.ijbiomac.2016.05.054.

33 RINAUDO, M. Chitin and chitosan: properties and applications. **Progress in Polymer Science**, v. 31, n. 7, p. 603–632, 2006.

34 YOUNES, I. *et al*. Influence of acetylation degree and molecular weight of homogeneous chitosans on antibacterial and antifungal activities. **International Journal of Food Microbiology**, v. 185, p. 57–63, 2014. DOI: 10.1016/j.ijfoodmicro.2014.04.029.

35 FOSTER, L. J. R. *et al*. Chitosan as a biomaterial: influence of degree of deacetylation on its physiochemical, material and biological properties. **PLoS ONE**, v. 10, n. 8, p. 1–22, 2015.

36 ILYAS, R. A. *et al*. Natural-fiber-reinforced chitosan, chitosan blends and their nanocomposites for various advanced applications. **Polymers**, v. 14, n. 5, 2022. DOI: 10.3390/polym14050874.

37 KARIMI, F. *et al*. Removal of metal ions using a new magnetic chitosan nano-bio-adsorbent; a powerful approach in water treatment. **Environmental Research**, v. 203, p. 111753, 2022. DOI: 10.1016/j.envres.2021.111753.

38 RAHMAN, N. A. *et al*. Chitosan as a paradigm for biopolymer electrolytes in solid-state dye-sensitised solar cells. **Polymer**, v. 230, p. 124092, 2021. DOI: 10.1016/j.polymer.2021.124092.

39 PAVINATTO, F. J. *et al*. Interaction of chitosan with cell membrane models at the air-water interface. **Biomacromolecules**, v. 8, n. 5, p. 1633–1640, 2007.

40 WYDRO, P.; KRAJEWSKA, B.; HĄC-WYDRO, K. Chitosan as a lipid binder: a Langmuir monolayer study of chitosan-lipid interactions. **Biomacromolecules**, v. 8, n. 8, p. 2611–2617, 2007.

41 PAVINATTO, F. J.; CASELI, L.; OLIVEIRA, O. N. Chitosan in nanostructured thin films. **Biomacromolecules**, v. 11, n. 8, p. 1897–1908, 2010.

42 CÁMARA, C. I. *et al*. Effect of chitosan on distearoylphosphatidylglycerol films at air/water and liquid/liquid interfaces. **Electrochimica Acta**, v. 94, p. 124–133, 2013. DOI: 10.1016/j.electacta.2013.01.137.

43 AHMED, I. *et al*. Chitosan-fatty acid interaction mediated growth of Langmuir monolayer and Langmuir-Blodgett films. **Journal of Colloid and Interface Science**, v. 514, p. 433–442, 2018. DOI: 10.1016/j.jcis.2017.12.037.

44 PEDRO, R. O. *et al*. Interaction of chitosan derivatives with cell membrane models in a biologically relevant medium. **Colloids and Surfaces B**: biointerfaces, v. 192, p. 111048, 2020. DOI: 10.1016/j.colsurfb.2020.111048.

45 WOŹNIAK, K.; JURAK, M.; WIĄCEK, A. E. Characterization of mixed langmuir monolayers of cyclosporine a with the phospholipid dppc at the chitosan subphase. **Progress on Chemistry and Application of Chitin and its Derivatives**, v. 25, p. 227–235, 2020. DOI:10.15259/PCACD.25.018.

46 PAVINATTO, A. *et al*. Experimental evidence for the mode of action based on electrostatic and hydrophobic forces to explain interaction between chitosans and phospholipid Langmuir monolayers. **Colloids and Surfaces B:** biointerfaces, v. 145, p. 201–207, 2016. DOI: 10.1016/j.colsurfb.2016.05.001.

47 PAVINATTO, A. *et al*. Low molecular-weight chitosans are stronger biomembrane model perturbants. **Colloids and Surfaces B:** biointerfaces, v. 104, p. 48–53, 2013. DOI: 10.1016/j.colsurfb.2012.11.047.

48 PAVINATTO, F. J. *et al*. Cholesterol mediates chitosan activity on phospholipid monolayers and langmuir-Blodgett films. **Langmuir**, v. 25, n. 17, p. 10051–10061, 2009.

49 PAVINATTO, F. J. *et al*. Probing chitosan and phospholipid interactions using Langmuir and Langmuir-Blodgett films as cell membrane models. **Langmuir**, v. 23, n. 14, p. 7666–7671, 2007.

50 CASELI, L. *et al*. Chitosan as a removing agent of β-Lactoglobulin from membrane models. **Langmuir**, v. 24, n. 8, p. 4150–4156, 2008.

51 KRAJEWSKA, B.; KYZIOŁ, A.; WYDRO, P. Chitosan as a subphase disturbant of membrane lipid monolayers. the effect of temperature at varying pH: II. DPPC and cholesterol. **Colloids and Surfaces A**: physicochemical and engineering aspects, v. 434, p. 359–364, 2013. DOI: 10.1016/j.colsurfa.2013.03.018.

52 KRAJEWSKA, B.; WYDRO, P.; KYZIOŁ, A. Chitosan as a subphase disturbant of membrane lipid monolayers. the effect of temperature at varying pH: I. DPPG. **Colloids and Surfaces A:** physicochemical and engineering aspects, v. 434, p. 349–358, 2013. DOI: 10.1016/j.colsurfa.2013.03.015.

53 KRAJEWSKA, B.; WYDRO, P.; JAŃCZYK, A. Probing the modes of antibacterial activity of chitosan. effects of pH and molecular weight on chitosan interactions with membrane lipids in Langmuir films. **Biomacromolecules**, v. 12, n. 11, p. 4144–4152, 2011.

54 ŁADNIAK, A.; JURAK, M.; WIĄCEK, A. E. The effect of chitosan/TiO2/hyaluronic acid subphase on the behaviour of 1,2-dioleoyl-sn-glycero-3-phosphocholine membrane. **Biomaterials Advances**, v. 138, p. 20–31, 2022. DOI: 10.1016/j.bioadv.2022.212934.

55 SZAFRAN, K.; JURAK, M.; WIĄCEK, A. E. Effect of chitosan on the interactions between phospholipid DOPC, cyclosporine A and lauryl gallate in the Langmuir monolayers. **Colloids and Surfaces A**: physicochemical and engineering aspects, v. 652, 2022. DOI: 10.1016/j.colsurfa.2022.129843.

56 ŁADNIAK, A.; JURAK, M.; WIĄCEK, A. E. Langmuir monolayer study of phospholipid DPPC on the titanium dioxide–chitosan–hyaluronic acid subphases. **Adsorption**, v. 25, p. 469–476, 2019. DOI: 10.1007/s10450-019-00037-1.

57 AVANTI POLAR LIPIDS. **Phospholipids**, 2020. Available from: https://avantilipids.com/product-category/phospholipids. Accessible at: 8 July 2020.

58 LE BRUN, A. P. *et al*. Structural characterization of a model Gram-Negative bacterial surface using lipopolysaccharides from rough strains of *Escherichia coli*. **Biomacromolecules**, v. 14, n. 6, p. 2014–2022, 2013.

59 HAC-WYDRO, K. *et al*. The influence of phospholipid structure on the interactions with nystatin, a polyene antifungal antibiotic. a Langmuir monolayer study. **Chemistry and Physics of Lipids**, v. 150, n. 2, p. 125–135, 2007.

60 SALAY, L. C. *et al*. Headgroup specificity for the interaction of the antimicrobial peptide tritrpticin with phospholipid Langmuir monolayers. **Colloids and Surfaces B**: biointerfaces, v. 100, p. 95–102, 2012. DOI: 10.1016/j.colsurfb.2012.05.002.

61 WYDRO, P.; WITKOWSKA, K. The interactions between phosphatidylglycerol and phosphatidylethanolamines in model bacterial membranes: the effect of the acyl chain length and saturation. **Colloids and surfaces B:** biointerfaces, v. 72, n. 1, p. 32–39, 2009.

62 PAVINATTO, F. J. **Interação entre quitosana e modelos de membrana celular** : filmes de Langmuir e Langmuir-Blodgett (LB). 2010. 163p. Tese (Doutorado em Interunidades Ciência e Engenharia de Materiais) - Escola de Engenharia de São Carlos, Instituto de Física de São Carlos, Instituto de Química de São Carlos, Universidade de São Paulo, São Carlos, 2010.

63 KSV NIMA. **Langmuir and Langmuir-Blodgett devices**: software manual all models revision 1.4. 2013. 117 p. Available from: https://www.ccmr.cornell.edu/wp-content/uploads/sites/2/2015/11/KSV-NIMA-LB-Software-Manual_v1.4.pdf. Accessible at: 30 Sept. 2022.

64 BRONIATOWSKI, M. *et al*. Grazing incidence diffraction and x-ray reflectivity studies of the interactions of inorganic mercury salts with membrane lipids in Langmuir monolayers at the air/water interface. **Journal of Physical Chemistry B**, v. 114, n. 29, p. 9474–9484, 2010.

65 COLD SPRING HARBOR PROTOCOLS. **Phosphate-buffered saline (PBS)**. 2006. Available from: http://cshprotocols.cshlp.org/content/2006/1/pdb.rec8247. Accessible at: 30 Sept. 2022.

66 JOCHELAVICIUS, K. *et al*. Chitosan effects on monolayers of zwitterionic, anionic and a natural lipid extract from *E. coli* at physiological pH. **Colloids and Surfaces B:** biointerfaces, v. 209, 2022. DOI: 10.1016/j.colsurfb.2021.112146.

67 STEINKOPF, S. *et al*. PH-dependent interaction of psychotropic drug with glycerophospholipid monolayers studied by the Langmuir technique. **Biophysical Chemistry**, v. 152, n. 1–3, p. 65–73, 2010.

68 WYDRO, P. The influence of cardiolipin on phosphatidylglycerol/phosphatidylethanolamine monolayers-studies on ternary films imitating bacterial membranes. **Colloids and Surfaces B**: biointerfaces, v. 106, p. 217–223, 2013. DOI: 10.1016/j.colsurfb.2013.01.053.

69 HOYO, J.; TORRENT-BURGUÉS, J.; TZANOV, T. Physical states and thermodynamic properties of model gram-negative bacterial inner membranes. **Chemistry and Physics of Lipids**, v. 218, p. 57–64, 2019. DOI: 10.1016/j.chemphyslip.2018.12.003.

70 ZERROUK, Z. *et al*. Inner membrane lipids of *Escherichia coli* form domains. **Colloids and Surfaces B**: biointerfaces, v. 63, n. 2, p. 306–310, 2008.

71 LÓPEZ-MONTERO, I. *et al*. High fluidity and soft elasticity of the inner membrane of *Escherichia coli* revealed by the surface rheology of model langmuir monolayers. **Langmuir**, v. 24, n. 8, p. 4065–4076, 2008.

72 WYDRO, P. The magnitude of condensation induced by cholesterol on the mixtures of sphingomyelin with phosphatidylcholines-study on ternary and quaternary systems. **Colloids and Surfaces B**: biointerfaces, v. 82, n. 2, p. 594–601, 2011.

73 VÁZQUEZ, R. F. *et al*. Impact of sphingomyelin acyl chain (16:0 vs 24:1) on the interfacial properties of Langmuir monolayers: a PM-IRRAS study. **Colloids and Surfaces B**: biointerfaces, v. 173, p. 549–556, 2019. DOI: 10.1016/j.colsurfb.2018.10.018.

74 LUNA, C. *et al*. Thermodynamics of monolayers formed by mixtures of phosphatidylcholine/phosphatidylserine. **Colloids and Surfaces B**: biointerfaces, v. 85, n. 2, p. 293–300, 2011.

75 DLUHY, R. A. *et al*. Vibrational spectroscopy of biophysical monolayers. Applications of IR and Raman spectroscopy to biomembrane model systems at interfaces. **Spectrochimica Acta Part A:** molecular and biomolecular spectroscopy, v. 51, n. 8, p. 1413–1447, 1995.

76 DYNAROWICZ-ŁĄTKA, P.; DHANABALAN, A.; OLIVEIRA JUNIOR, O. N. Modern physicochemical research on Langmuir monolayers. **Advances in Colloid and Interface Science**, v. 91, n. 2, p. 221–293, 2001.

77 SORLIER, P.; VITON, C.; DOMARD, A. Relation between solution properties and degree of acetylation of chitosan: role of aging. **Biomacromolecules**, v. 3, n. 6, p. 1336–1342, 2002.

78 FOLLMANN, H. D. M. *et al*. Extent of shielding by counterions determines the bactericidal activity of N,N,N-trimethyl chitosan salts. **Carbohydrate Polymers**, v. 137, p. 418–425, 2016. DOI: 10.1016/j.carbpol.2015.10.083.